Comprehensive Modelling of the Middle and Upper Atmospheres

1995 CEDAR Tutorial

Kevin Hamilton

Why comprehensive modelling?

Brief description of what is involved in constructing a "comprehensive meteorological" model of the atmosphere - one particular model GFDL "SKYHI" model

Very brief description of SKYHI tropospheric simulation

15 Minute summary of key issues in stratospheric meteorology:

-radiative equilibrium
-effects of gravity waves on the mean circulation
-Rossby wave breaking and the "surf zone"

Aspects of SKYHI stratospheric simulation

Explicitly simulated upward gravity wave flux in SKYHI (including experiments to examine tropospheric excitation of such waves)

Simulated mechanical heating of mesosphere

Note: No diurnal cycle in the calculations discussed here

Making a "Comprehensive" General Circulation Model

Need a basic numerical scheme to solve some version of the Navier-Stokes equations (normally assume hydrostatic balance) for a rotating sphere with an irregular lower boundary

Also need explicit solution to continuity equations for water vapor and any other trace constituents considered

Need computation of radiative heating rates given the solar zenith angle and the temperature and distribution of absorbers throughout the atmospheric column

Need subgroup-scale damping parameterizations (eddy viscosity - vertical mixing should depend on vertical stability)

Need parameterizations for the interaction of atmosphere with the surface - (unresolved drag, evaporation, sensible heat exchange)

Parameterizations of condensation and precipitation

Some model (or prescription) of ground hydrology

Computation of chemical sources/sinks for any trace constituents considered

*Typically all electromagnetic effects are ignored

GFDL "SKYHI" Troposphere-Stratosphere-Mesosphere General Circulation Model

Comprehensive GCM for the atmosphere from the ground to 0.01 mb (~80 km)

Discretized on a latitude-longitude grid and over 40 levels in the vertical

1^{o}x1.2^{o}, 2^{o}x2.4^{o}, 3^{o}x3.6^{o} versions

Realistic land-sea distribution and topography

Realistic radiative transfer with full annual cycle of solar radiation

Prescribed ozone amounts (with a local temperature dependence) and prescribed cloud fields

Prognostic water vapor equation with parameterization of evaporation, condensation, surface water storage and runoff etc.

Dry and moist convective adjustment

Ri dependent subgrid scale vertical mixing

Prescribed annual cycle of sea surface temperature

Simple N_2O chemistry in standard runs - are developing a fairly complete ozone chemistry (Lori Perliski)

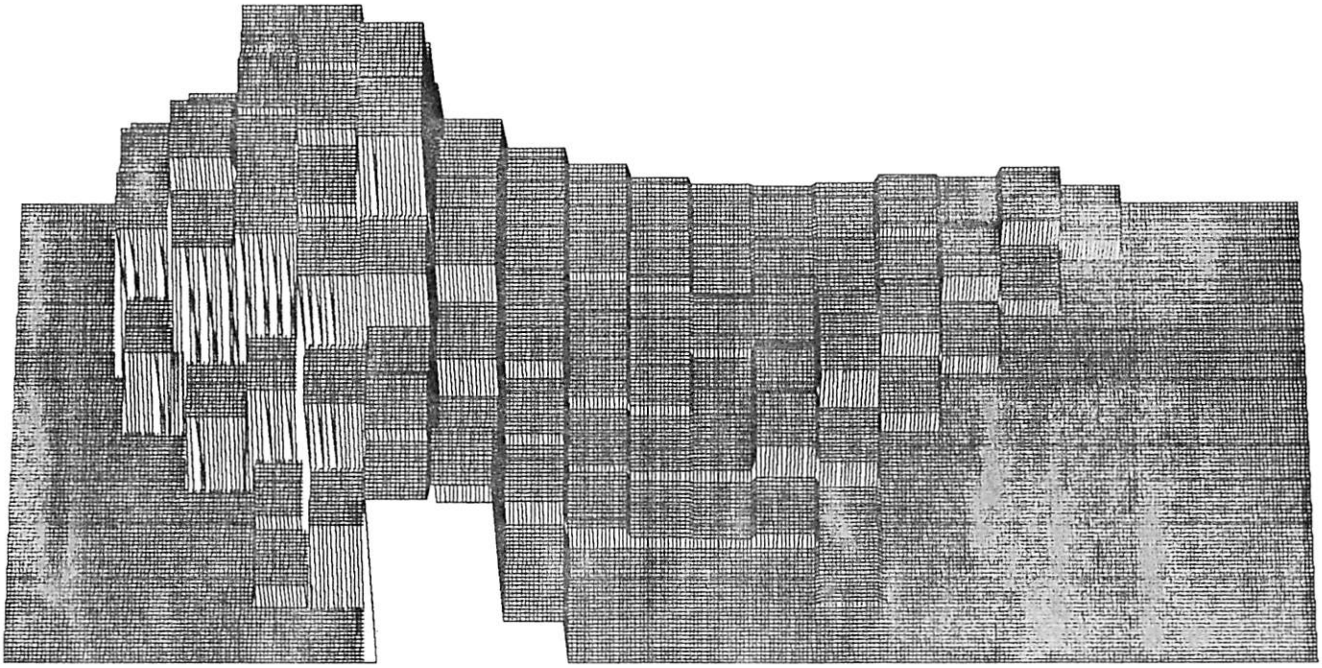

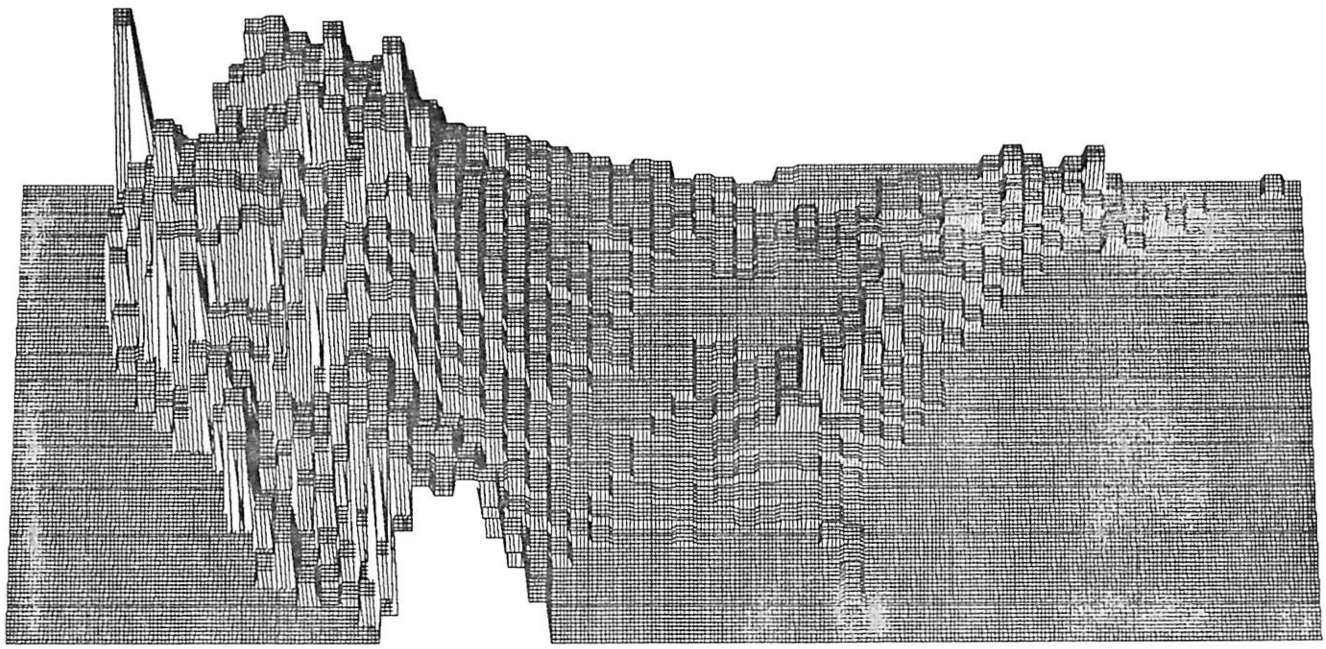

Problems (particularly important for MLT region)

Radiative transfer assumes LTE so we ignore non-LTE effects in computing emission of CO_2 and we ignore airglow, chemical heating

No diurnal cycle in constituents (notably O_3)

No electromagnetic effects

DJF U200

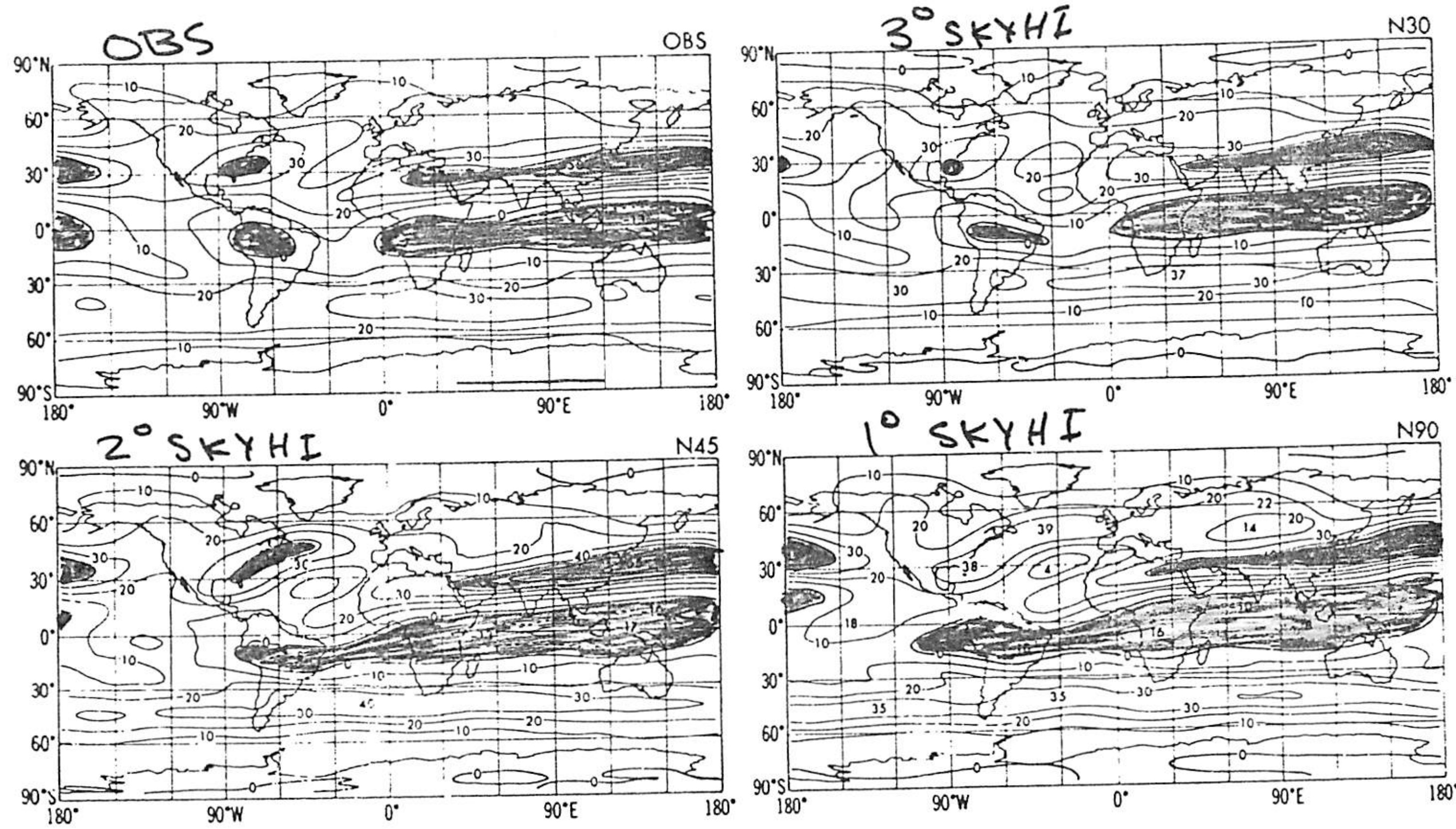

MULTIYEAR AVERAGE OF DJF MEAN EAST-WEST WIND

AT 200 mb (~10 km)

- easterly winds
- westerly winds > 40 m/s

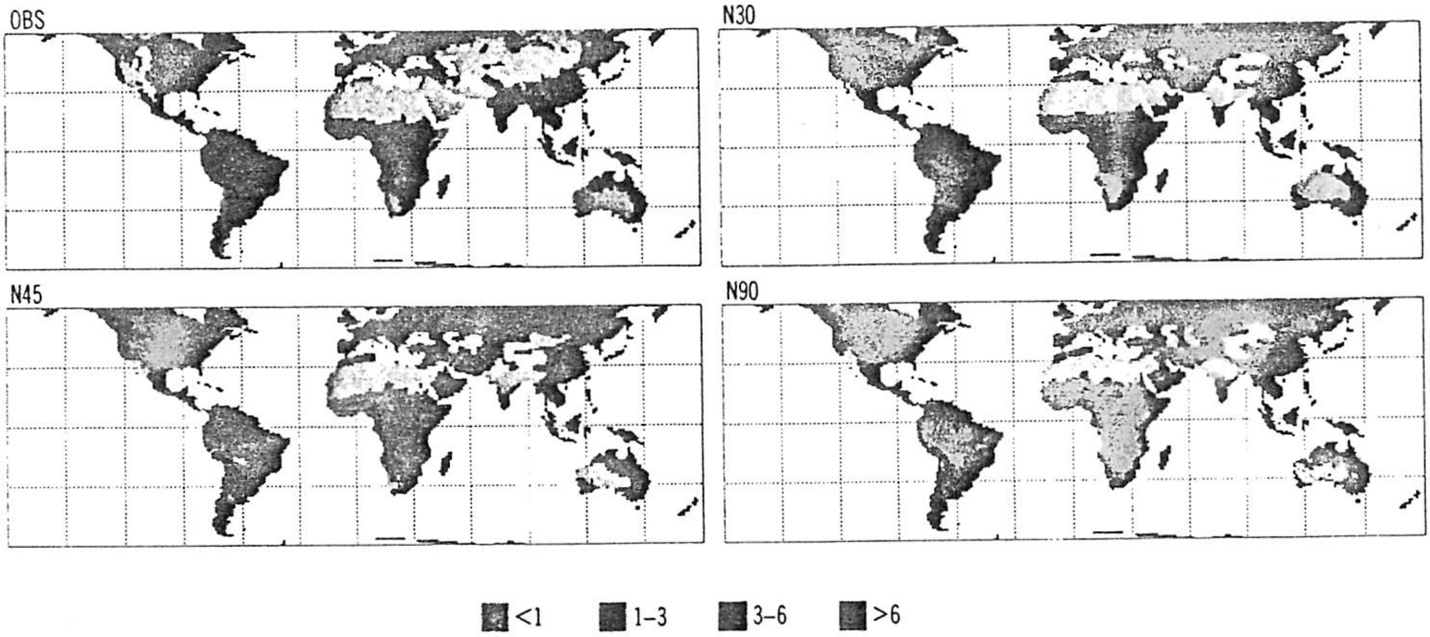

Fig. 8. Annual mean precipitation rate climatologies from observations and from the model control runs. The key to the shading is labelled in mm-day-1. Results shown only for land areas equatorward of 60° latitude. The model fields are unsmoothed and plotted at the model resolution in each case. The observations are from Legates and Willmott (1990), but their 0.5°x0.5° data has been averaged into a 1°x1.2° grid boxes before plotting.

Fig. 8

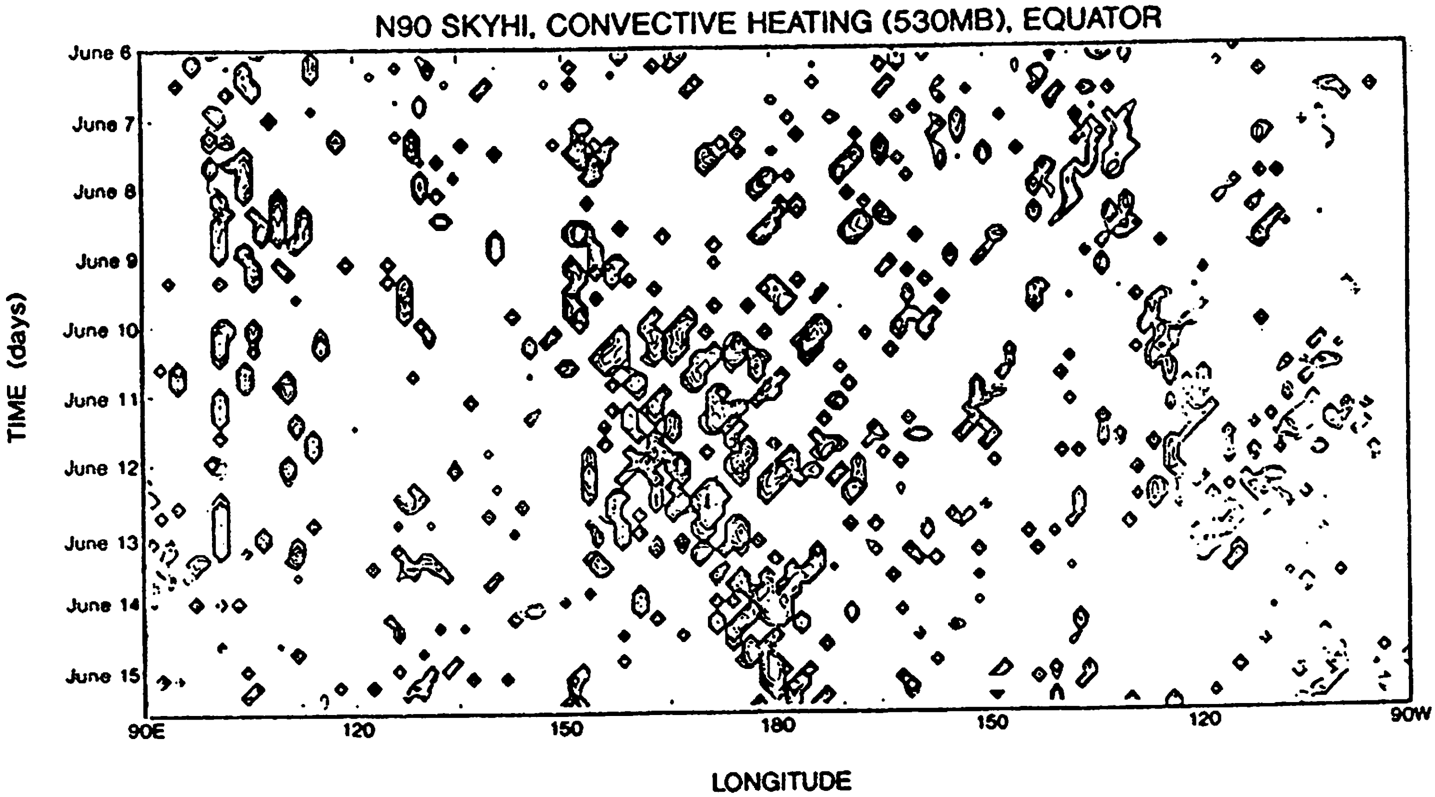
N90 SKYHI, CONVECTIVE HEATING (530MB), EQUATOR
TIME (days)
June 6
June 7
June 8
June 9
June 10
June 11
June 12
June 13
June 14
June 15
90E
120
150
180
150
120
90W
LONGITUDE

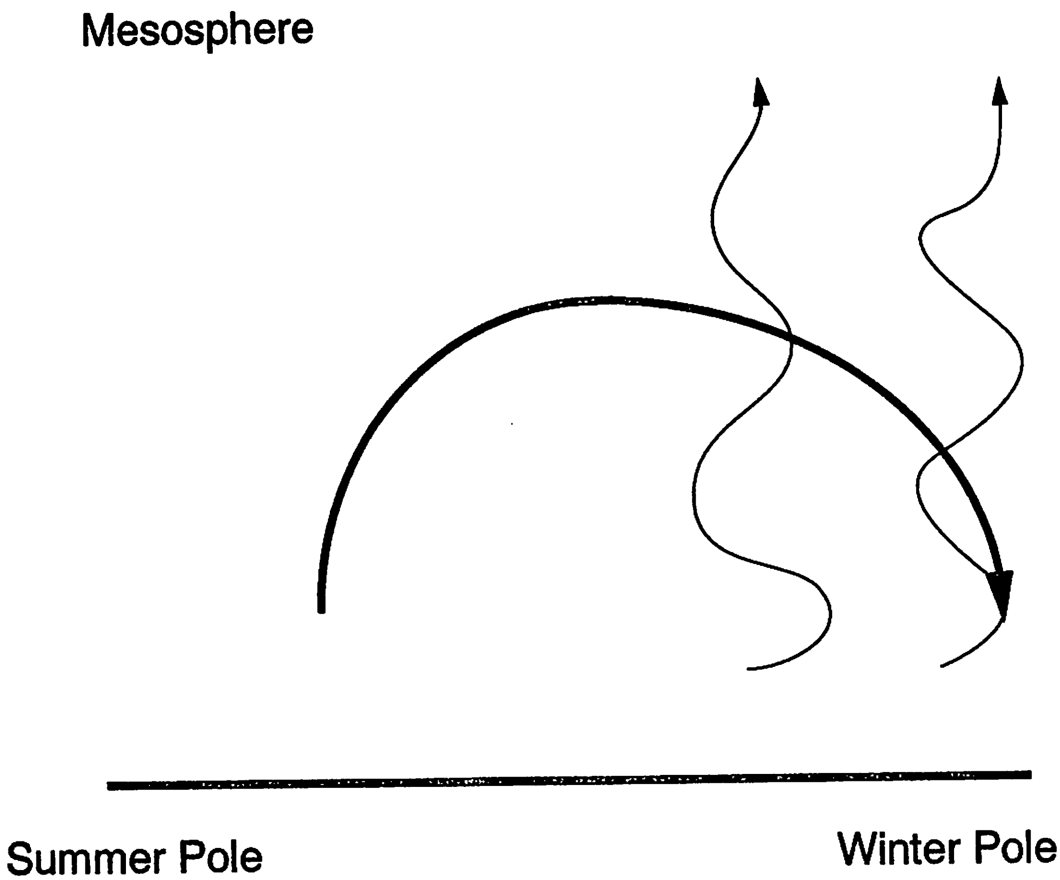
Mesosphere
Summer Pole
Winter Pole

$$\overline{\quad} = \int_0^L dx \qquad a = \bar{a} + a'$$

$$\cancel{\frac{\partial \bar{v}}{\partial t}} - f\bar{v} = -\frac{1}{\bar{\rho}}\frac{\partial}{\partial z}\rho\overline{u'w'} - \frac{\partial}{\partial y}\overline{u'v'}$$

$$\cancel{\frac{\partial \bar{T}}{\partial t}} + N^2\bar{w} = Q = \alpha(T - T_{rad})$$

$$\frac{\partial \bar{v}}{\partial y} + \frac{1}{\rho}\frac{\partial}{\partial z}\overline{\rho w} = 0$$

$$f\bar{u} = -\frac{1}{\rho}\frac{\partial \bar{P}}{\partial y}$$

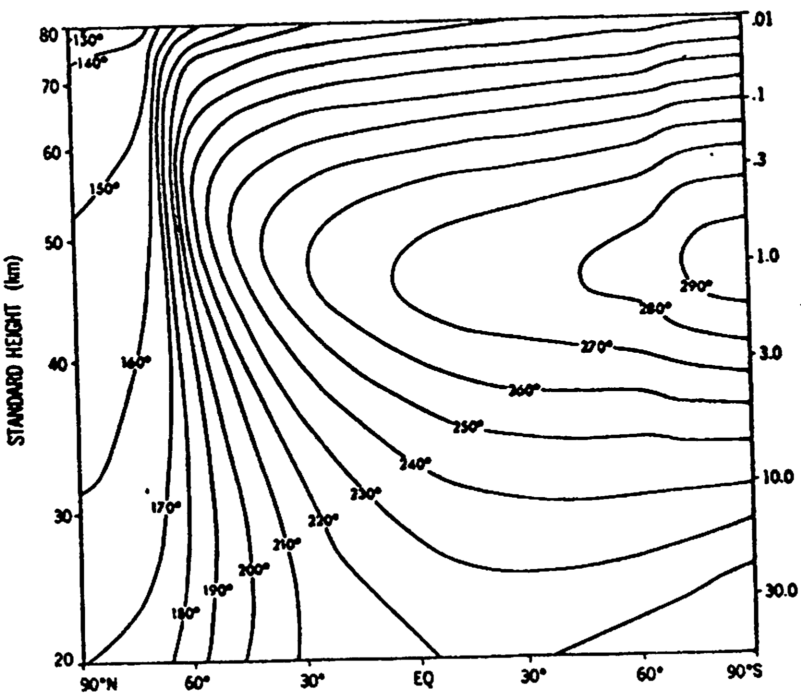

STANDARD HEIGHT (km)
P (mb)
150°
140°
150°
160°
170°
180°
190°
200°
210°
220°
230°
240°
250°
260°
270°
280°
290°
90°N
60°
30°
EQ
30°
60°
90°S

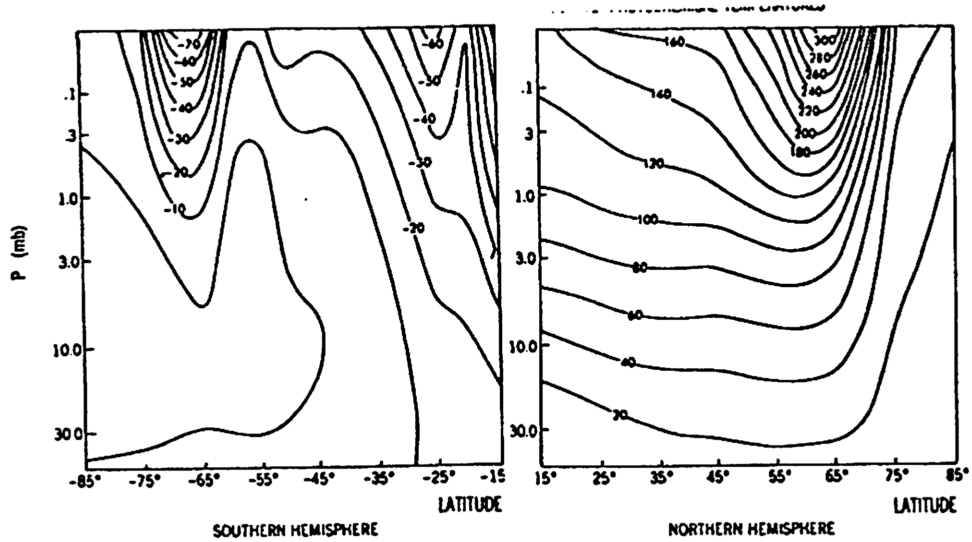

P (mb)
LATITUDE
SOUTHERN HEMISPHERE
LATITUDE
NORTHERN HEMISPHERE

GRADIENT WIND FOR JAN. 15th
RADIATIVE–PHOTOCHEMICAL TEMPERATURES

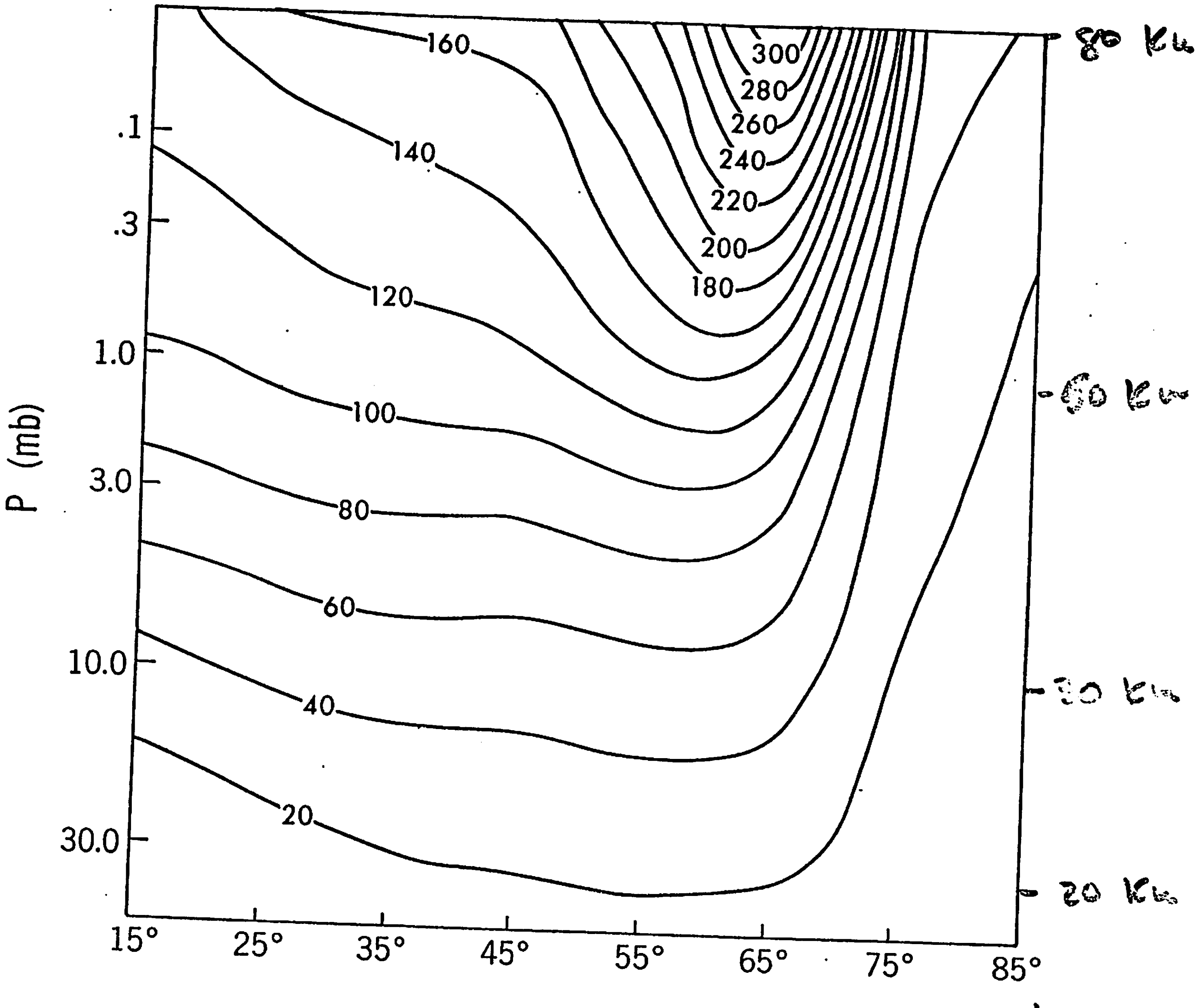

NORTHERN HEMISPHERE

Steady, linear, 2D, WKB gravity waves

$$u', w', T' \sim e^{i(kx + mz - \omega t)}$$

Take $\omega > 0$

Then $k > 0 \rightarrow$ westerly phase speed

For upward energy propagation $m < 0$

Then $\overline{u'w'} > 0$

And when waves dissipate $-\frac{\partial}{\partial z} \rho \overline{u'w'} > 0$

$$C_{gz} = \frac{(\omega - k\bar{u})^2}{N k}$$

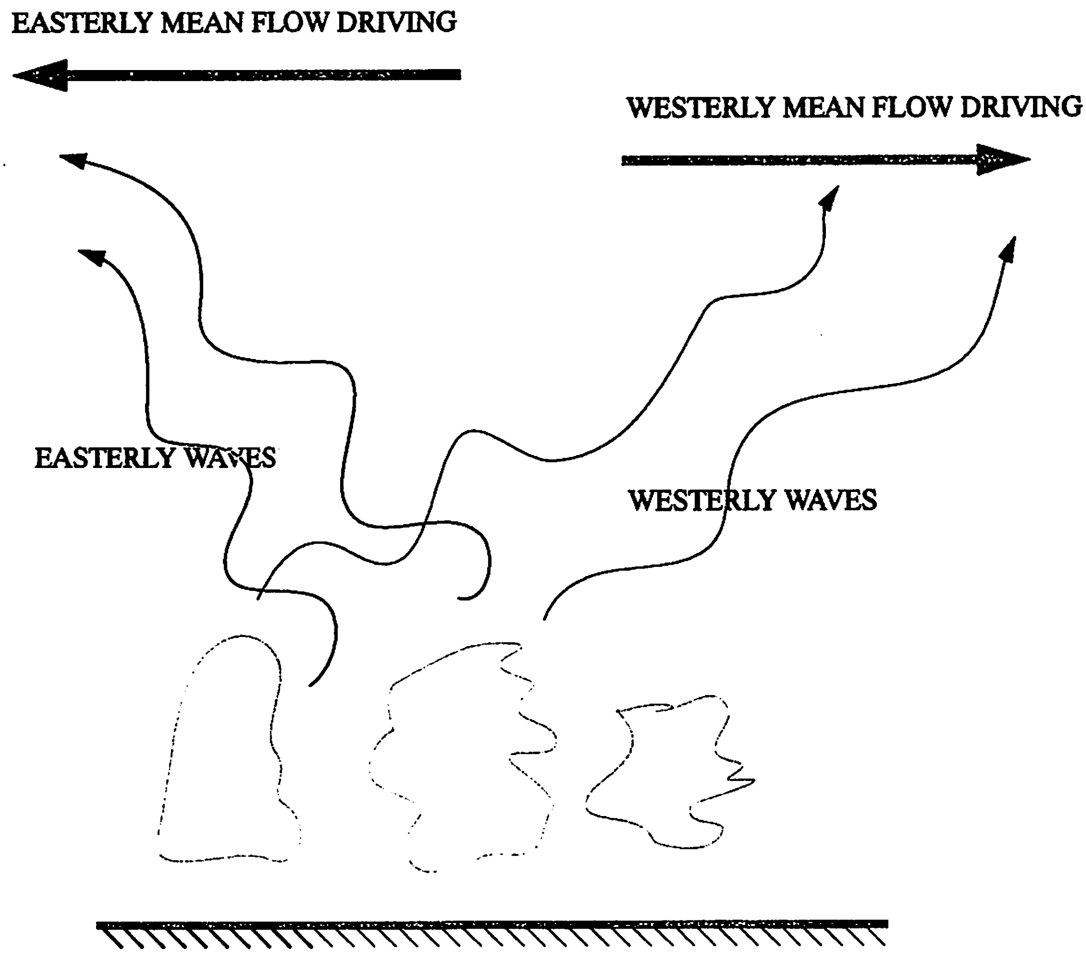
EASTERLY MEAN FLOW DRIVING
WESTERLY MEAN FLOW DRIVING
EASTERLY WAVES
WESTERLY WAVES

$q = f + \nabla^2 \psi$ $\quad\quad$ $u = -\dfrac{\partial \psi}{\partial y}$ $\quad$ $v = +\dfrac{\partial \psi}{\partial x}$

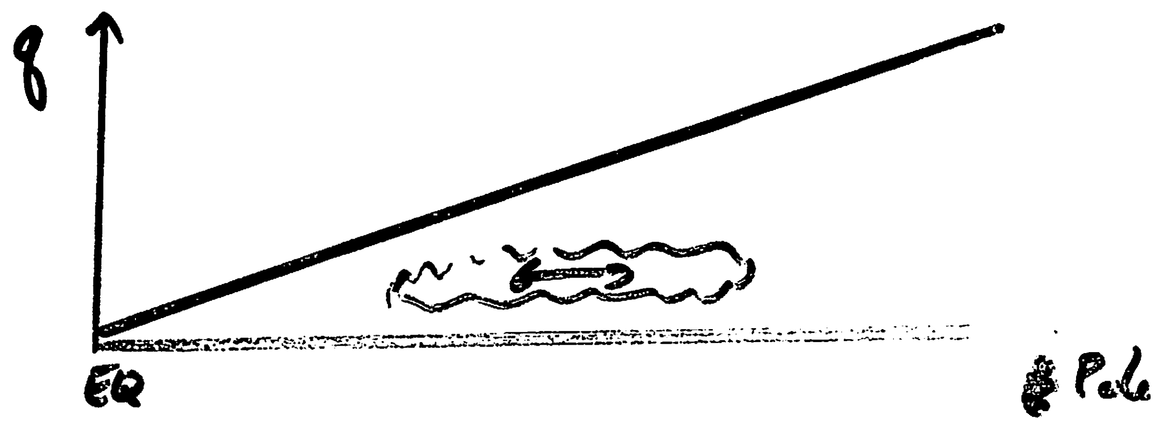

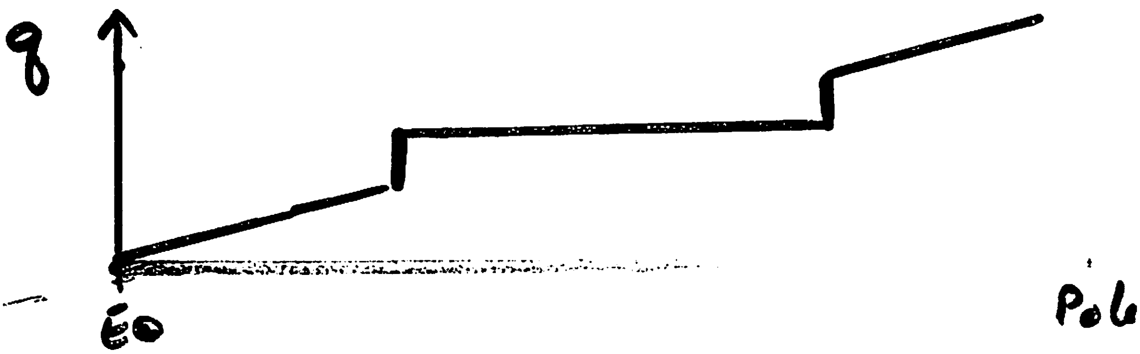

$$\overline{v'q'} < 0$$

$\Longleftarrow$

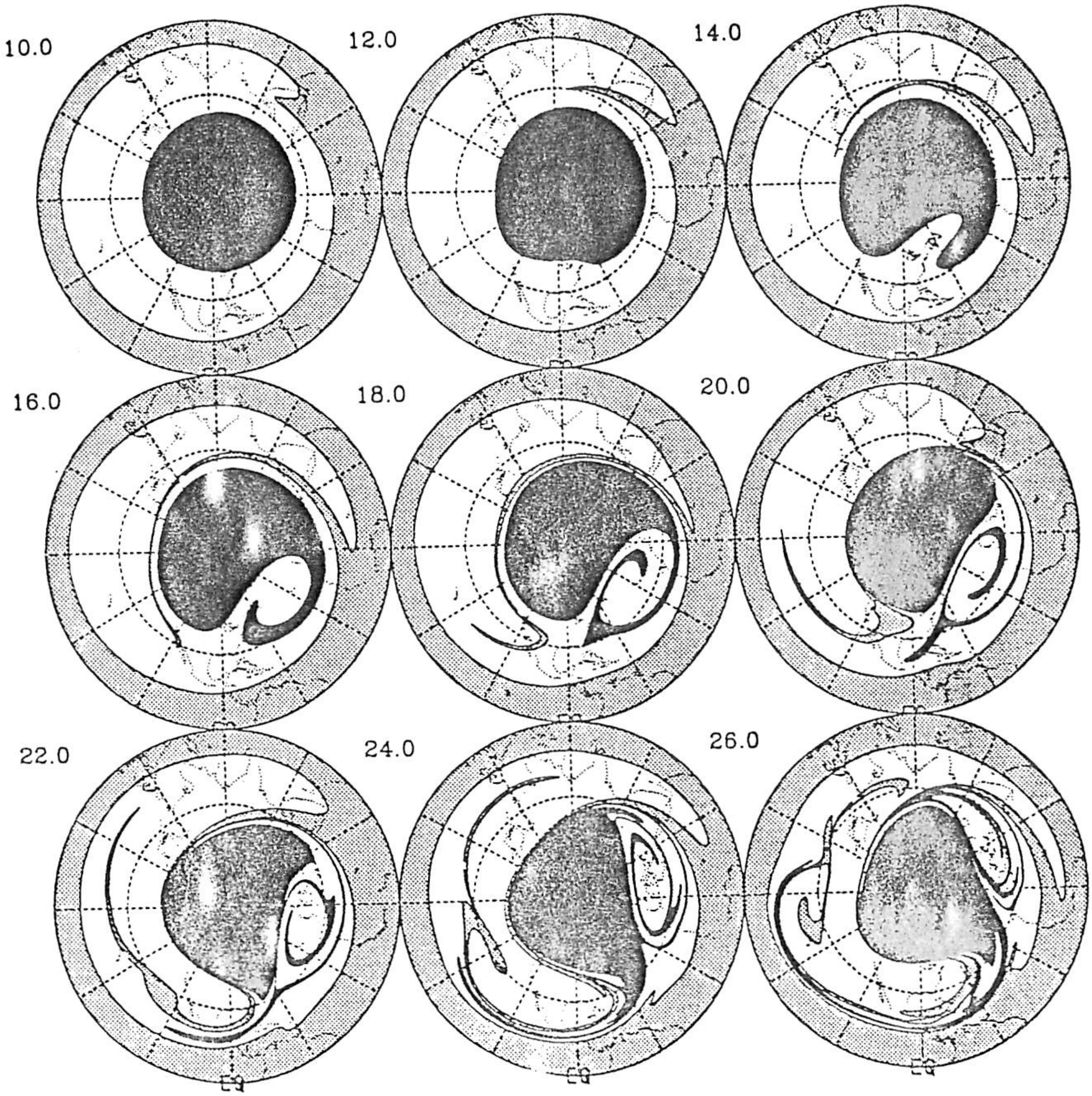

10.0
12.0
14.0
16.0
18.0
20.0
22.0
24.0
26.0
EQ
EQ
EQ

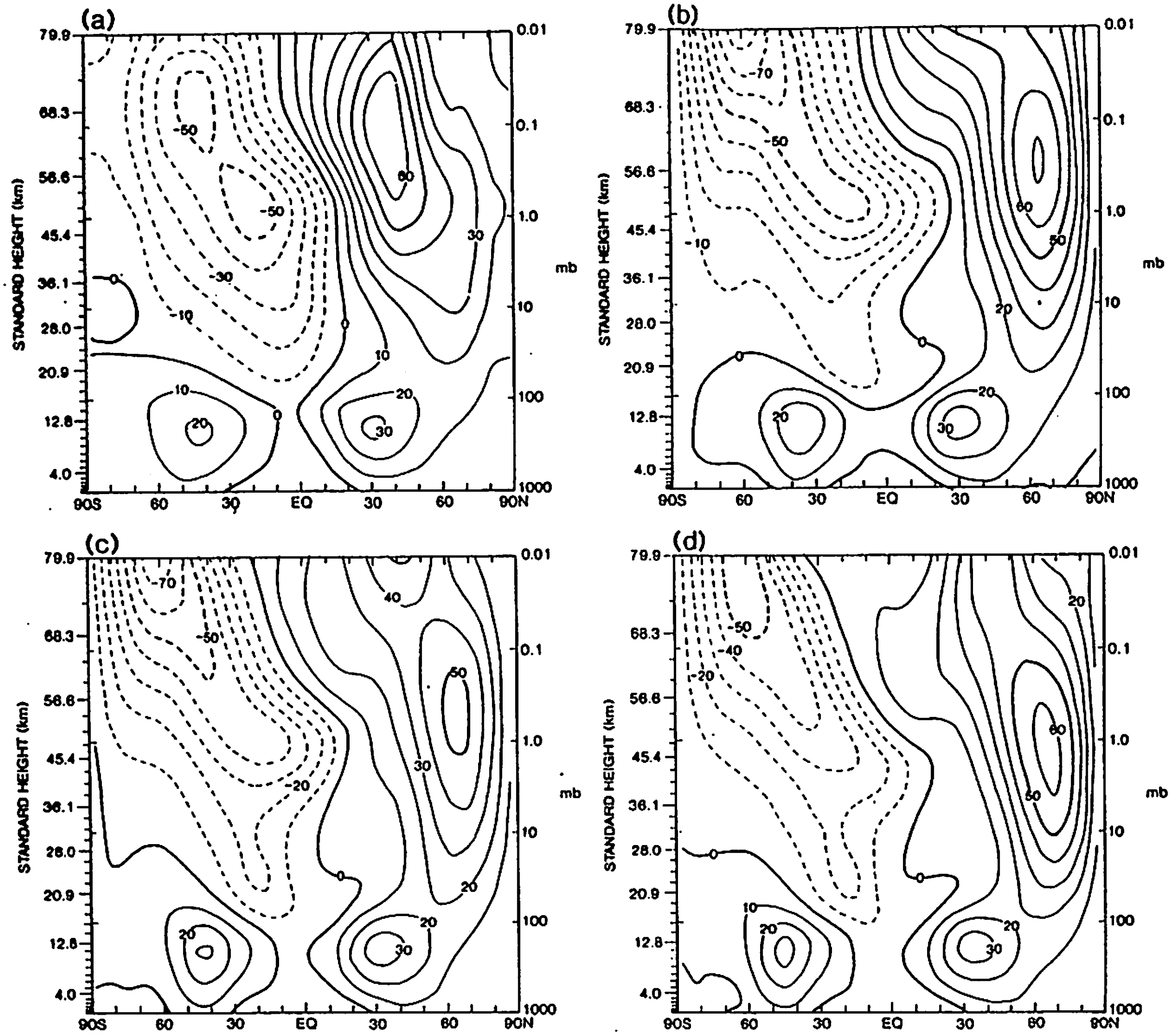

Figure 1. December-February mean zonally-averaged zonal wind climatologies from observations and from the model control runs. The contour interval is 10 m-s^{-1} and dashed contours denote easterly winds. The tick marks on the left show the locations of the 40 SKYHI model levels. Results from (a) observations (Fleming et al., 1988), (b) a ten-year average of the 3^{o}x3.6^{o} SKYHI model simulation, (c) a two-year average of the 2^{o}x2.4^{o} model simulation, and (d) a two-year average of the 1^{o}x1.2^{o} simulation.

$$\overline{v'q'} = \overline{\frac{\partial\psi}{\partial x}\nabla^2\psi} = \underbrace{\overline{\frac{\partial\psi}{\partial x}\frac{\partial^2\psi}{\partial x^2}}}_{0} + \overline{\frac{\partial\psi}{\partial x}\frac{\partial^2\psi}{\partial y^2}}$$

$\rightarrow$ But
$$\overline{\frac{\partial\psi}{\partial x}\frac{\partial^2\psi}{\partial x^2}} = \overline{\frac{1}{2}\frac{\partial}{\partial x}\left[\left(\frac{\partial\psi}{\partial x}\right)^2\right]} = 0$$

$$-\frac{\partial}{\partial y}\overline{u'v'} = \overline{-\frac{\partial}{\partial y}\left(-\frac{\partial\psi}{\partial x}\frac{\partial\psi}{\partial y}\right)} = \overline{\frac{\partial}{\partial y}\left(\frac{\partial\psi}{\partial x}\frac{\partial\psi}{\partial y}\right)}$$

$$= \overline{\frac{\partial\psi}{\partial x}\frac{\partial^2\psi}{\partial y^2}} + \overline{\frac{\partial\psi}{\partial y}\frac{\partial}{\partial x}\left(\frac{\partial\psi}{\partial y}\right)}$$

$$= \overline{\frac{\partial\psi}{\partial x}\frac{\partial^2\psi}{\partial y^2}} + \overline{\frac{1}{2}\frac{\partial}{\partial x}\left[\left(\frac{\partial\psi}{\partial y}\right)^2\right]} = 0$$

$$\overline{v'q'} = -\frac{\partial}{\partial y}\overline{u'v'}$$

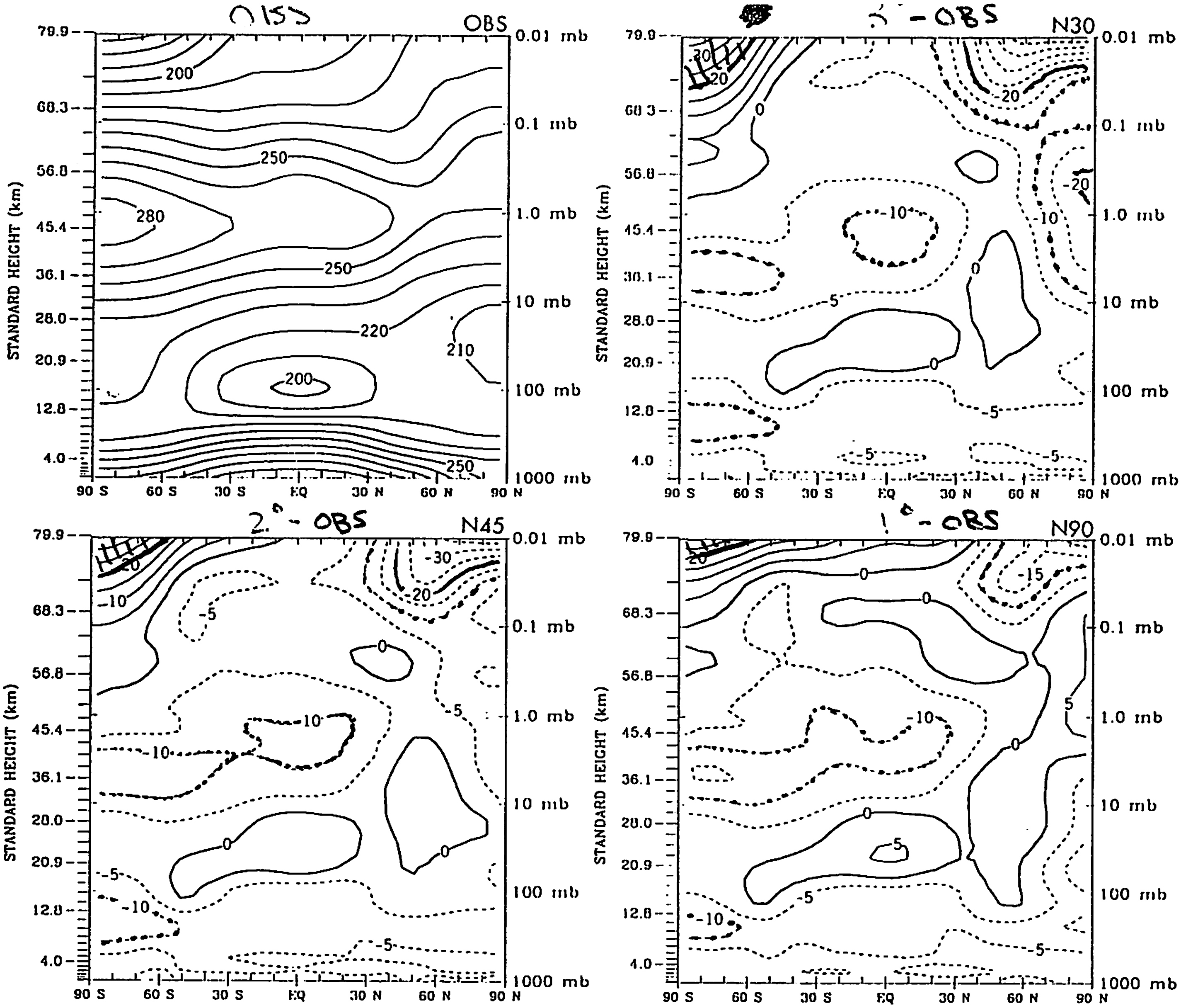

···· −10°

— −20°

■ > 20°

DJF mean temperature.

Fig. 27

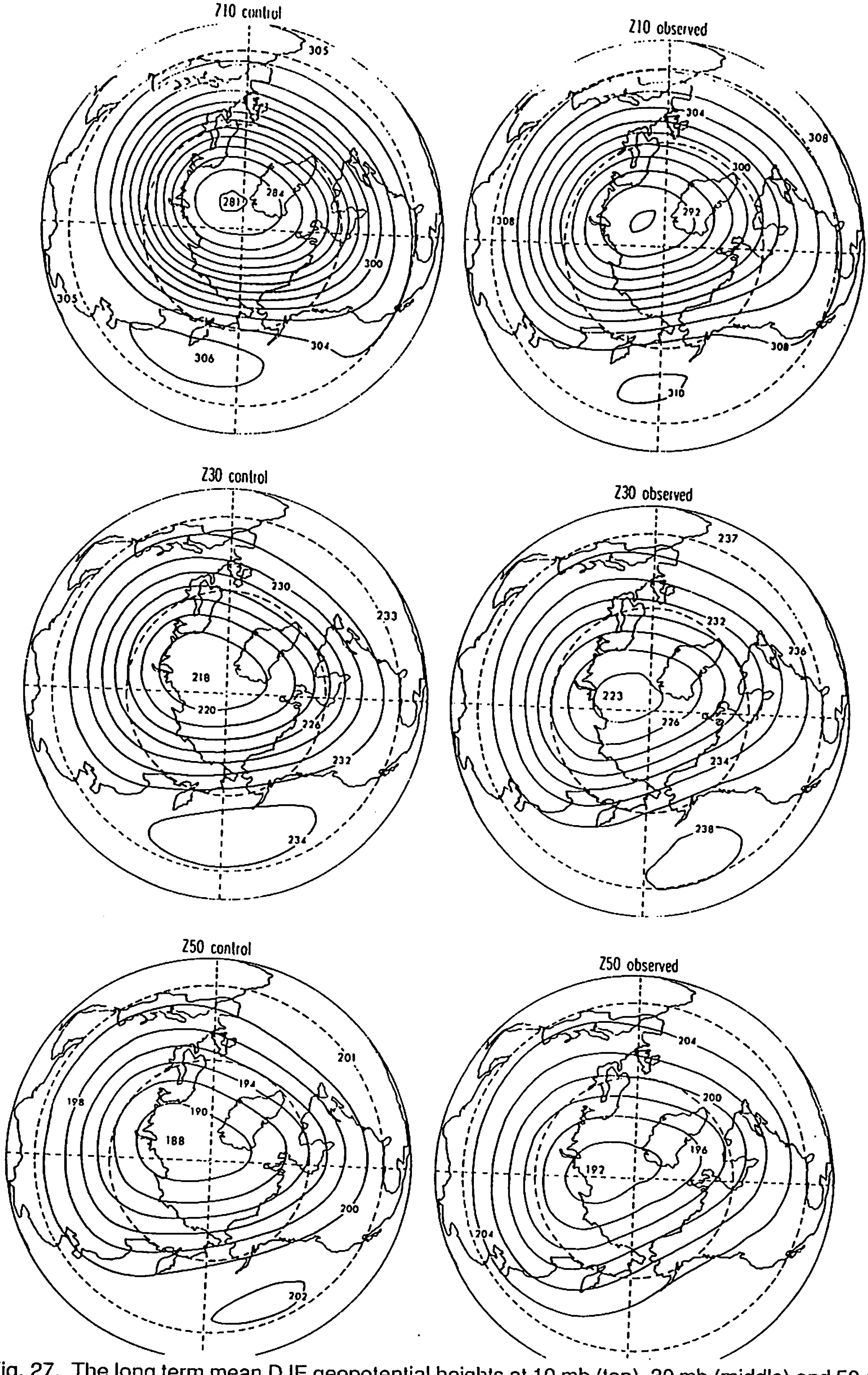

Fig. 27. The long term mean DJF geopotential heights at 10 mb (top), 30 mb (middle) and 50 mb (bottom) from the N30 SKYHI simulation (left) and observations (right). The contour labels are in 100's of m and the contour interval is 200 m. The dashed circles show 30°N and 60°N.

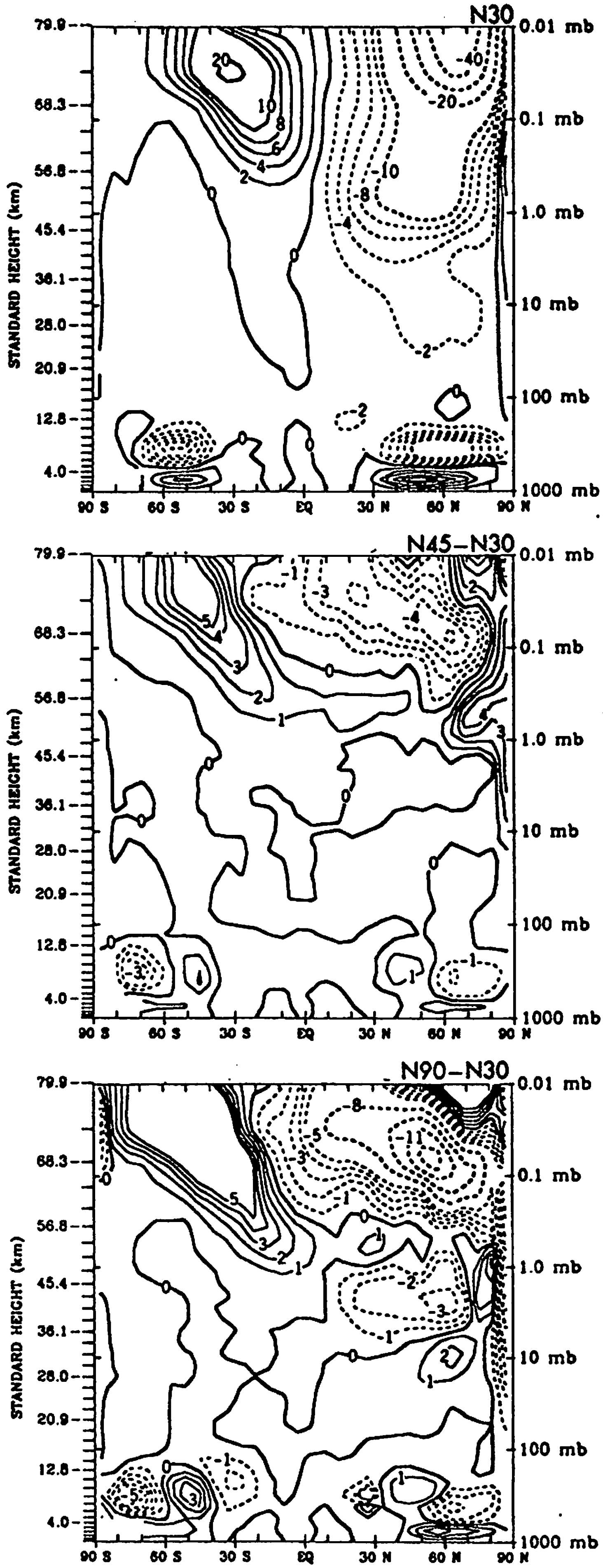

N30
N45-N30
N90-N30
STANDARD HEIGHT (km)
79.9
68.3
56.8
45.4
36.1
28.0
20.9
12.8
4.0
0.01 mb
0.1 mb
1.0 mb
10 mb
100 mb
1000 mb
90 S
60 S
30 S
EQ
30 N
60 N
90 N

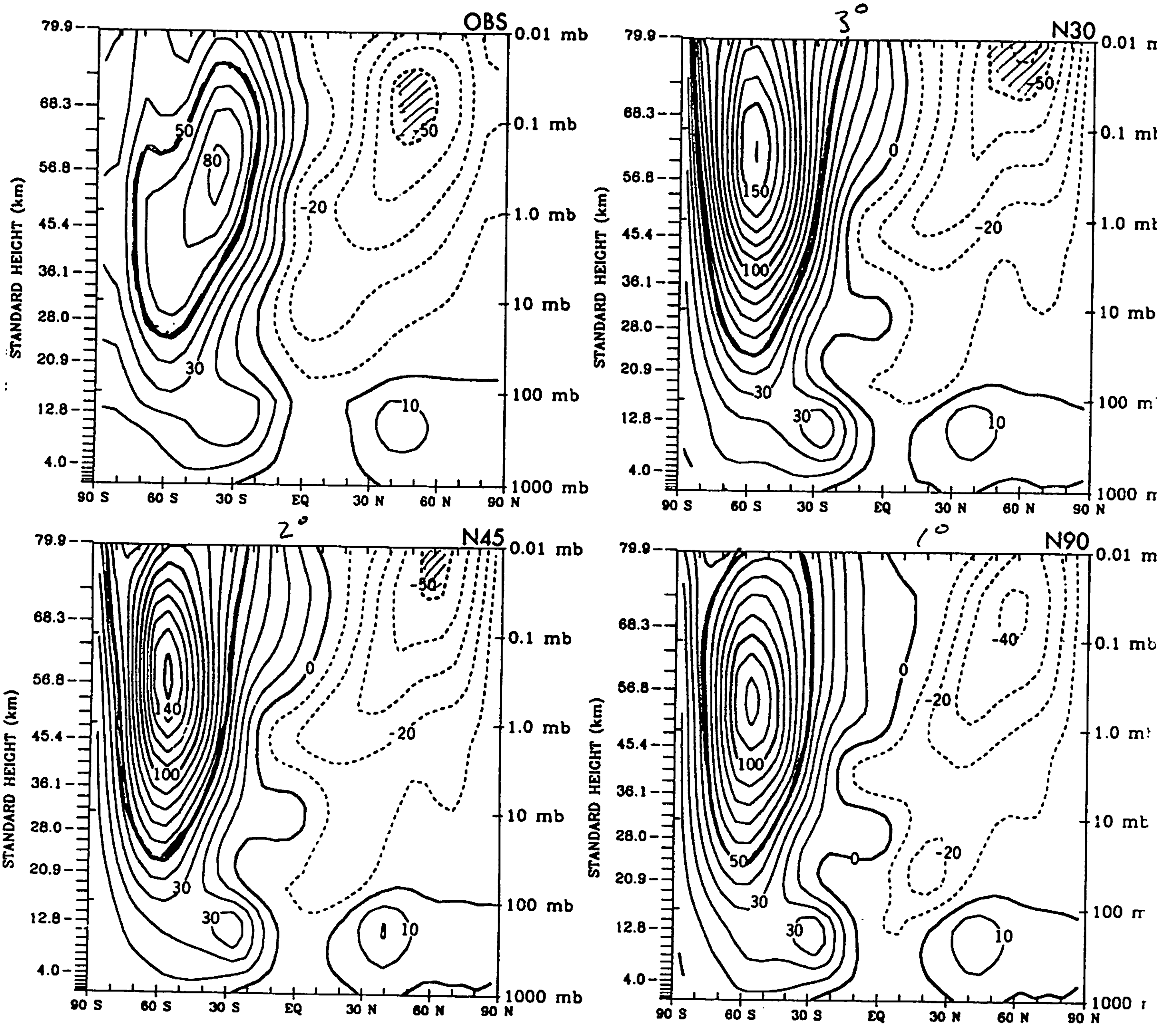
OBS
3°
N30
2°
N45
1°
N90
STANDARD HEIGHT (km)
79.9
68.3
56.8
45.4
36.1
28.0
20.9
12.8
4.0
0.01 mb
0.1 mb
1.0 mb
10 mb
100 mb
1000 mb
90 S
60 S
30 S
EQ
30 N
60 N
90 N
50
80
-20
-50
30
10
150
100
0
140
-40

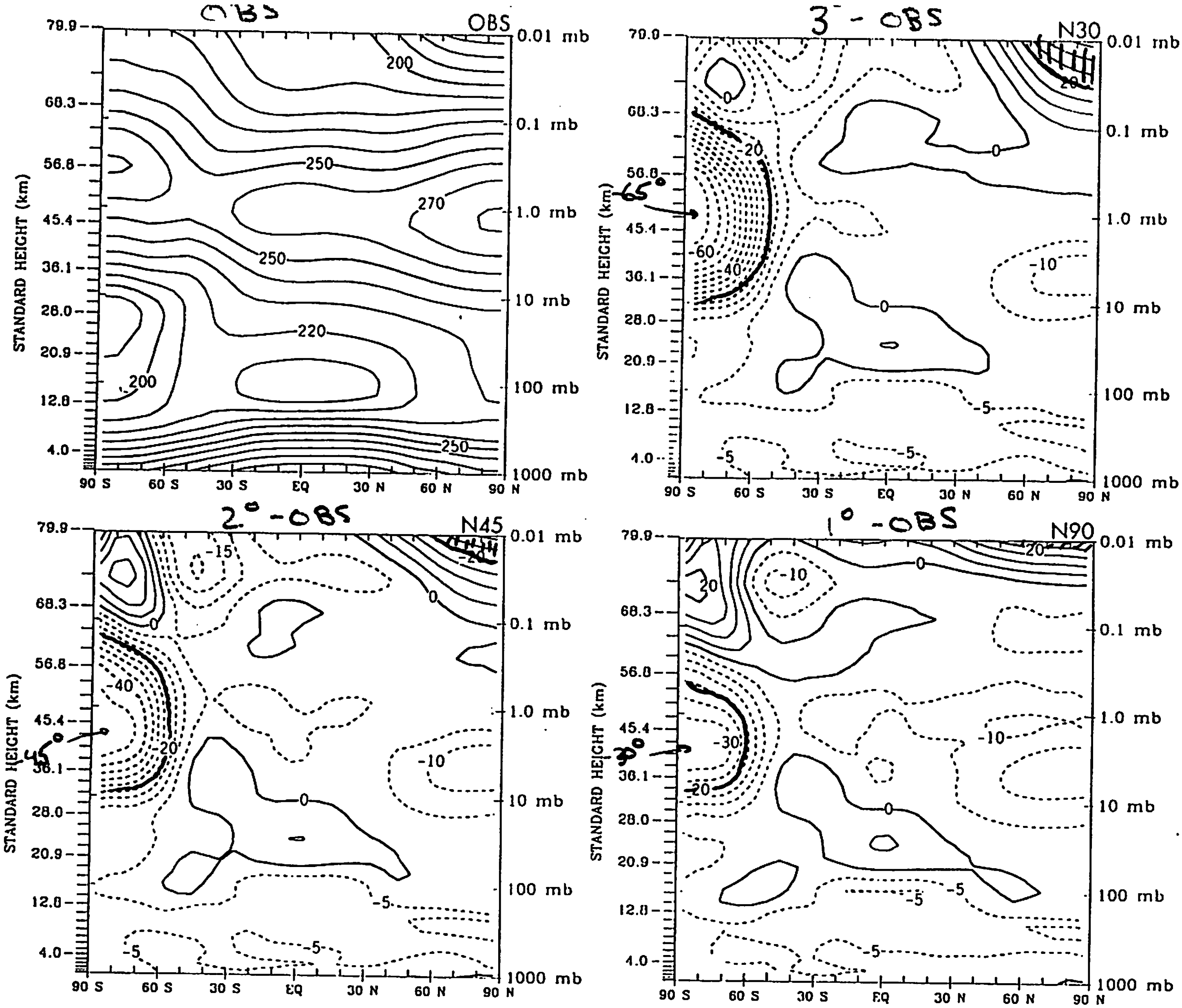

JJA temperature

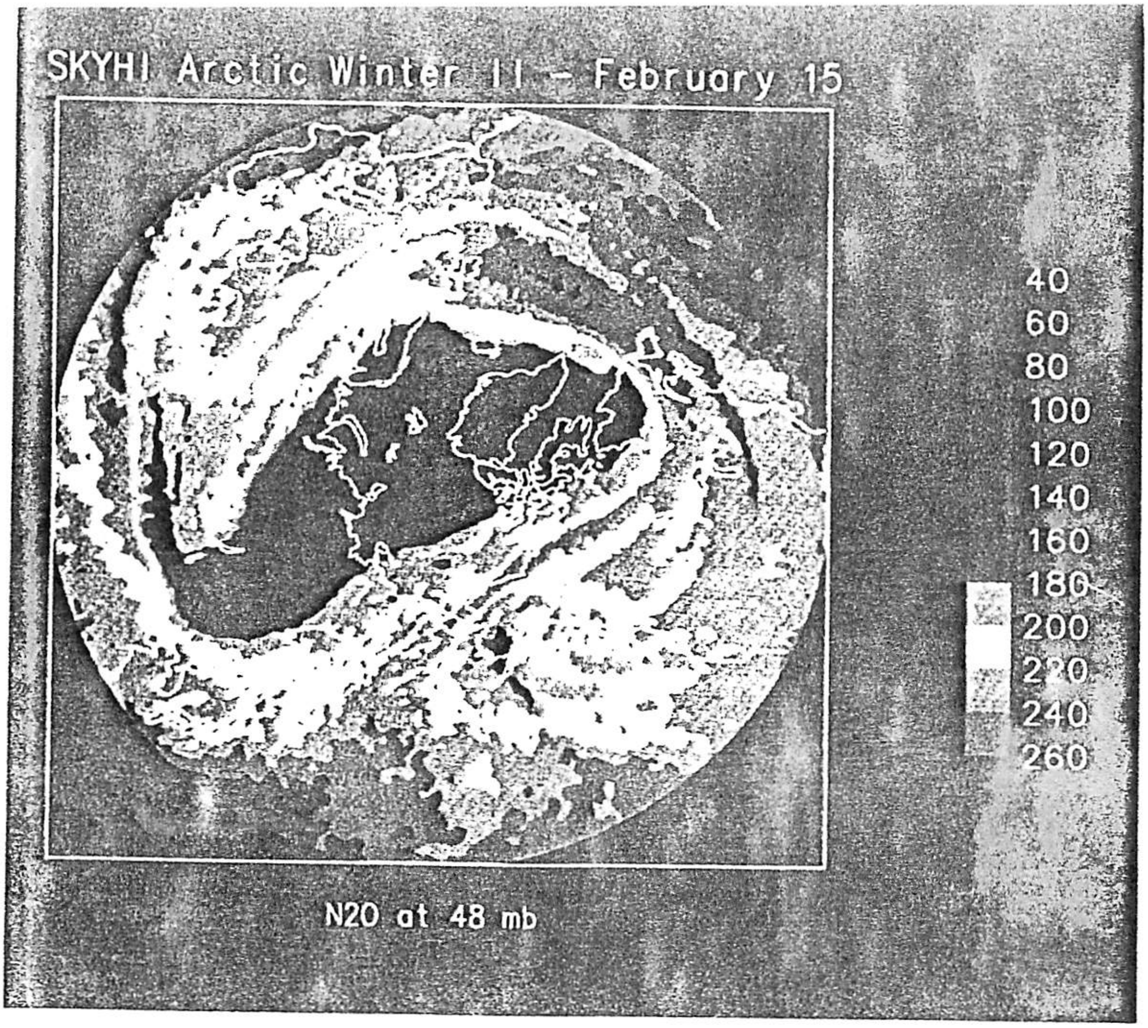

Plate 3. North polar satellite view of SKYHI N_2O at 48 mbar on model date February 15. A filament of vortex edge air (dark green) is being sheared away from the vortex over Europe and Asia, and higher mixing ratios (yellow) are intruding poleward of the filament. Note the high density of contours at the vortex edge.

It has wind speed maxima comparable to the AAOE wind is in close agreement with the analysis of *Schoeberl et al*

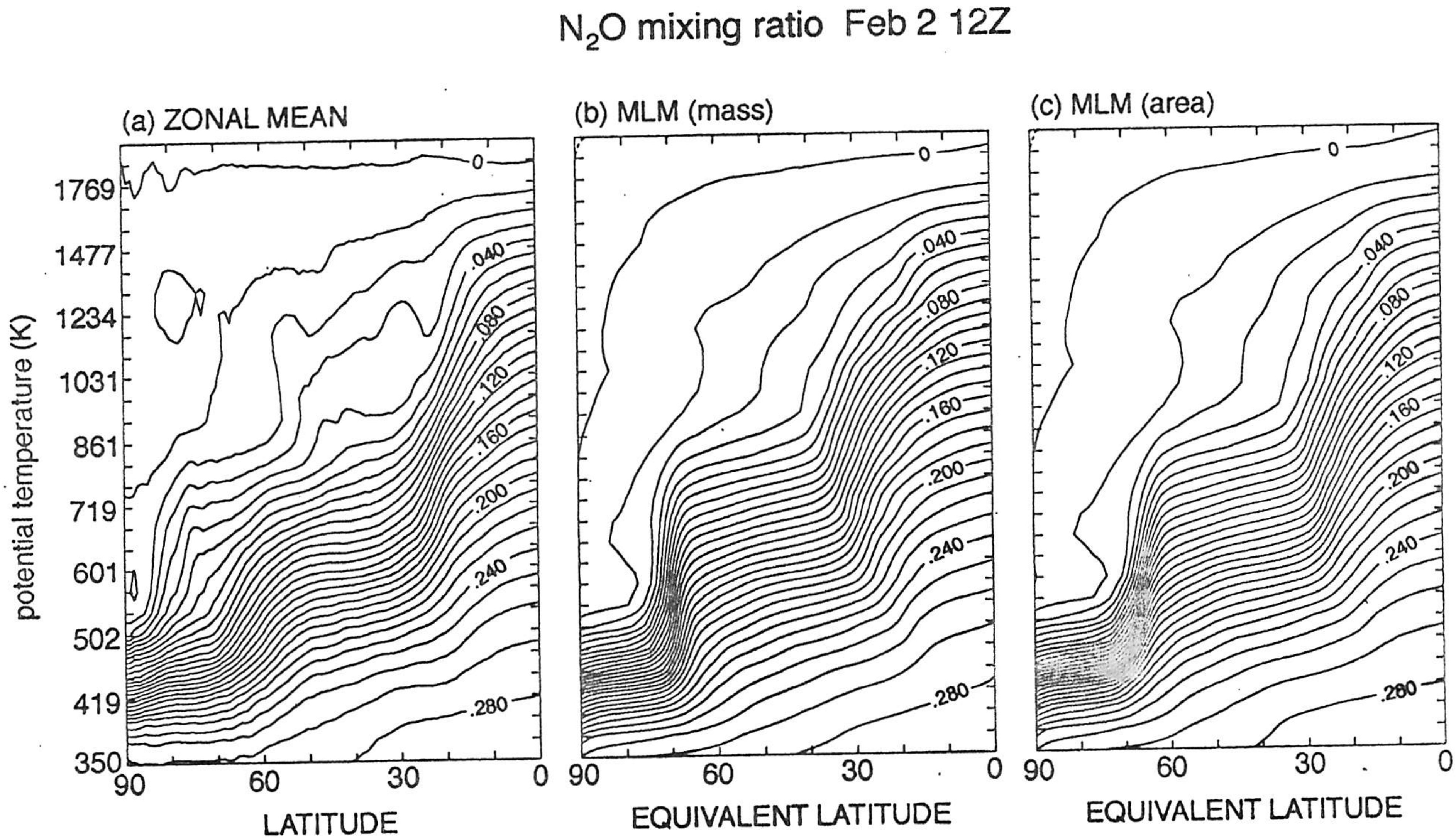

Fig.2 (a) Zonally averaged N2O mixing ratio in the northern hemisphere stratosphere, simulated by the GFDL SKYHI GCM (N90 resolution). The figure is an instantaneous snapshot at 12Z, February 2, 1984 (model year) plotted as a function of latitude and potential temperature (logarithmic scale). The corresponding height increases approximately uniformly from 10 to 50km. The contour interval is 0.01 ppm.

(b) The same instantaneous N2O field as (a) but based on the MLM analysis, plotted as a function of the equivalent latitude and potential temperature. The abscissa is the equivalent latitude defined by (2.11).

(c) Same as (b) but using the area analysis of Butchart and Remsberg (1986).

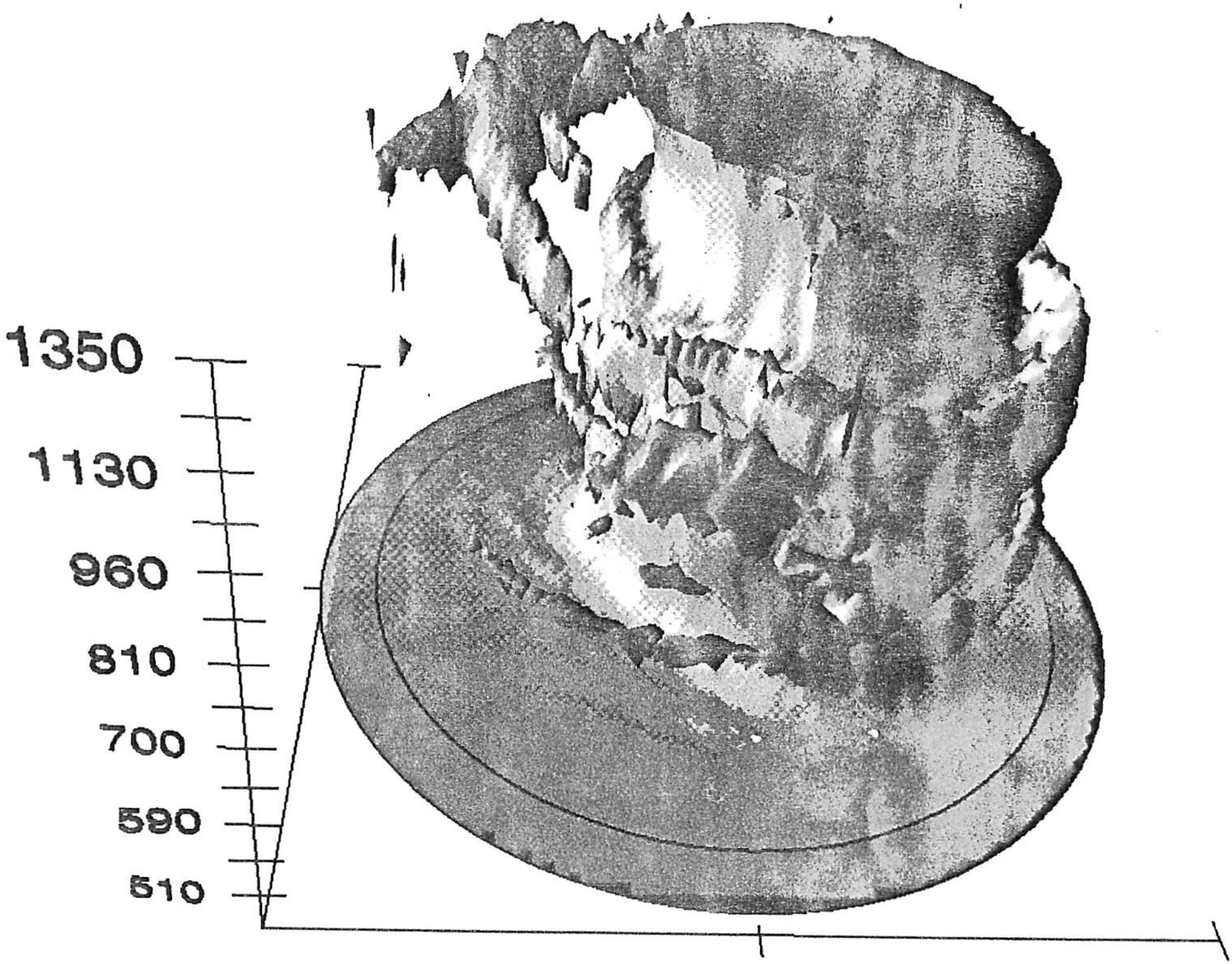
1350
1130
960
810
700
590
510

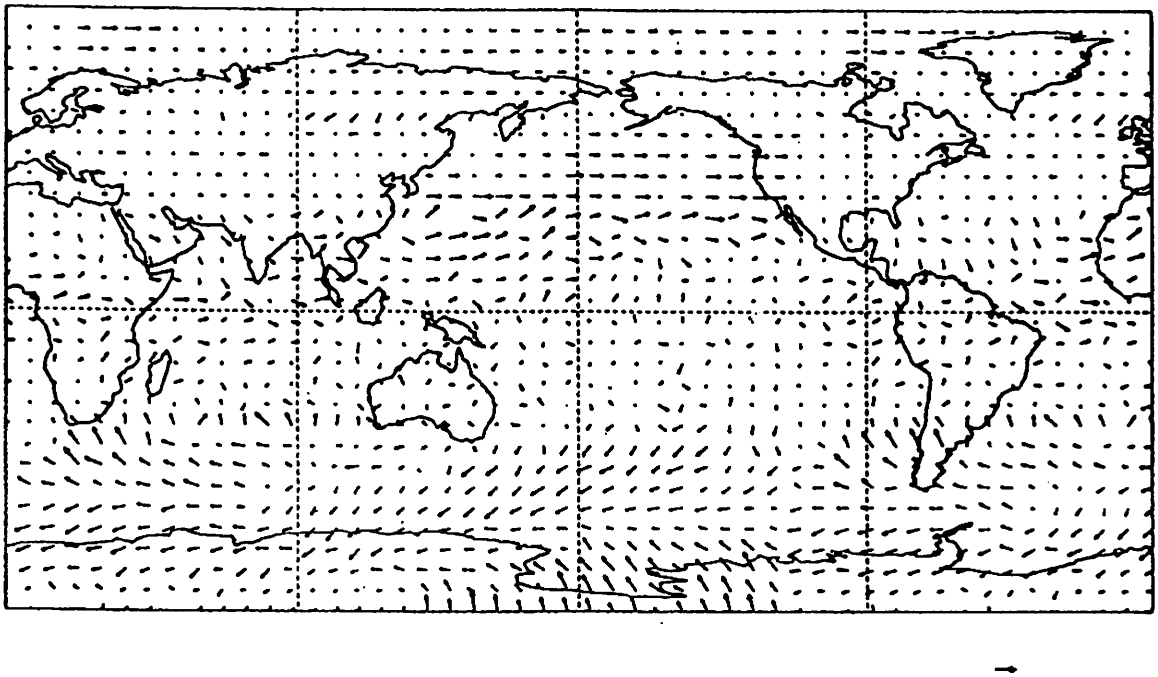

Figure 3. An instantaneous snapshot of the horizontal wind field at 0.0308 mb simulated in the 2^ox2.4^o SKYHI model at 12 GMT on February 15 during a long control run. Note that vectors are plotted only for every ninth grid point (*i.e.* 6^ox7.2^o resolution). The length of the vector shown at the lower right corner represents 100 m-s^{-1}.

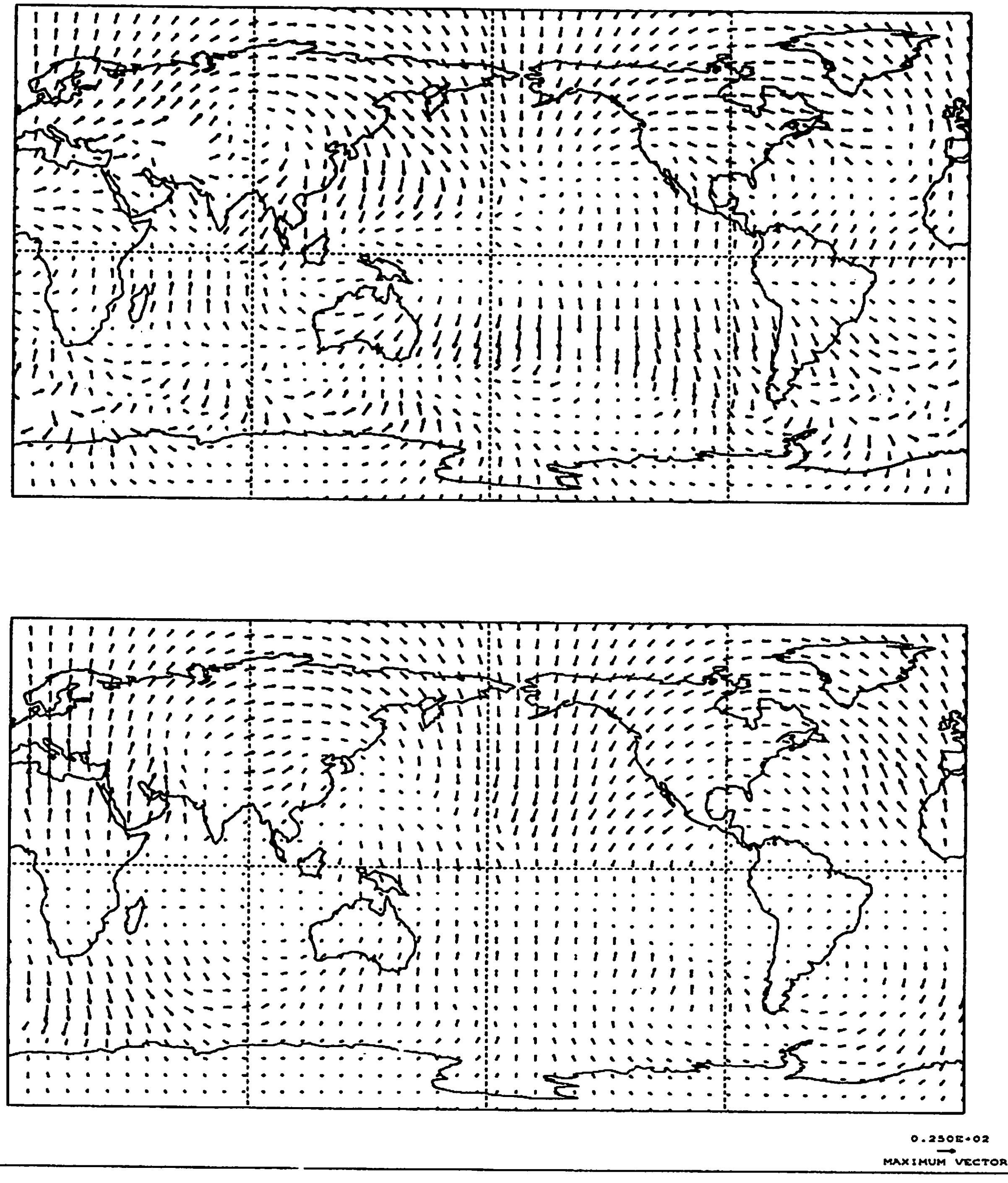
0.250E+02
MAXIMUM VECTOR

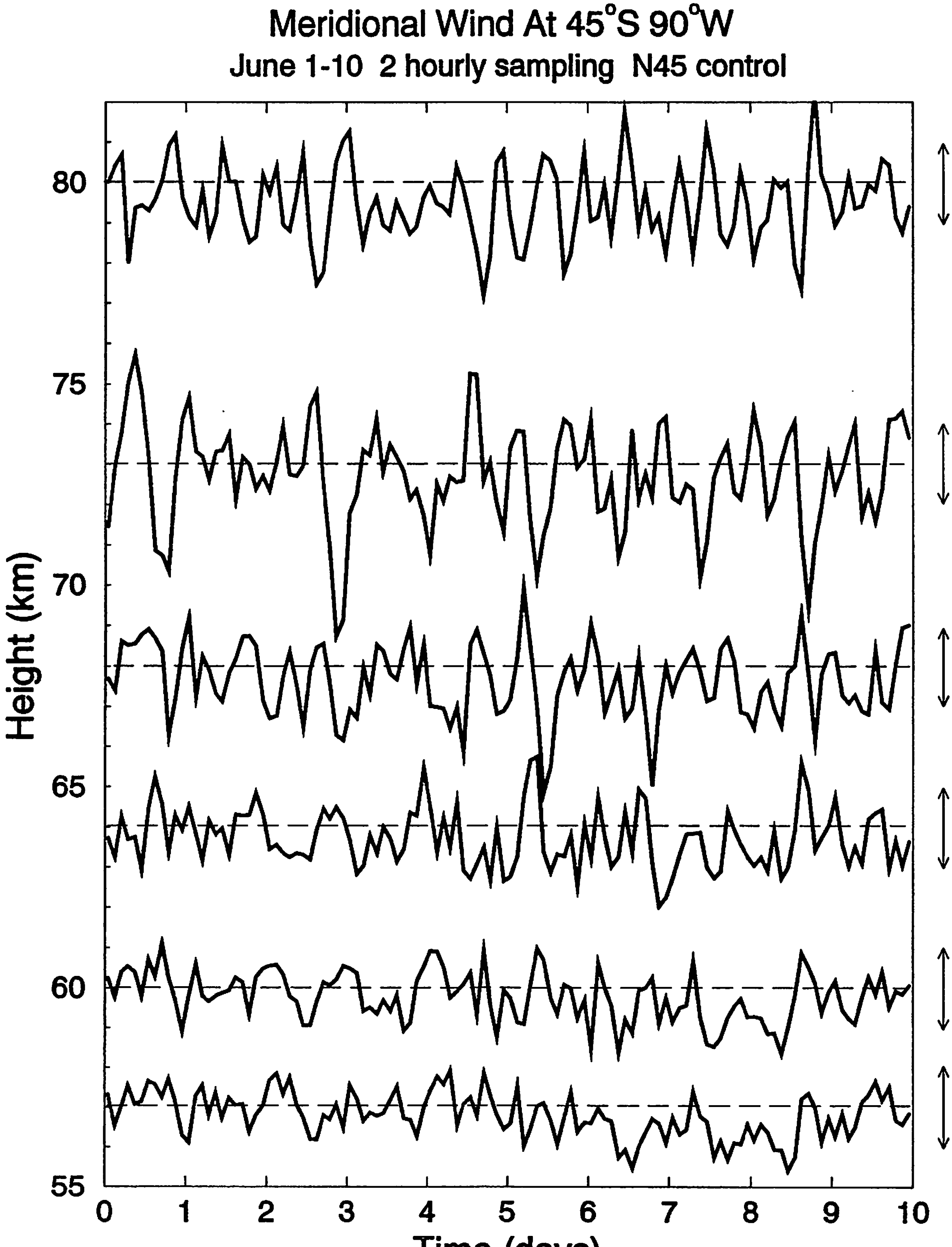

Meridional Wind At 45°S 90°W
June 1-10 2 hourly sampling N45 control
Height (km)
80
75
70
65
60
55
0
1
2
3
4
5
6
7
8
9
10
Time (days)
arrow denotes 40 m-s-1

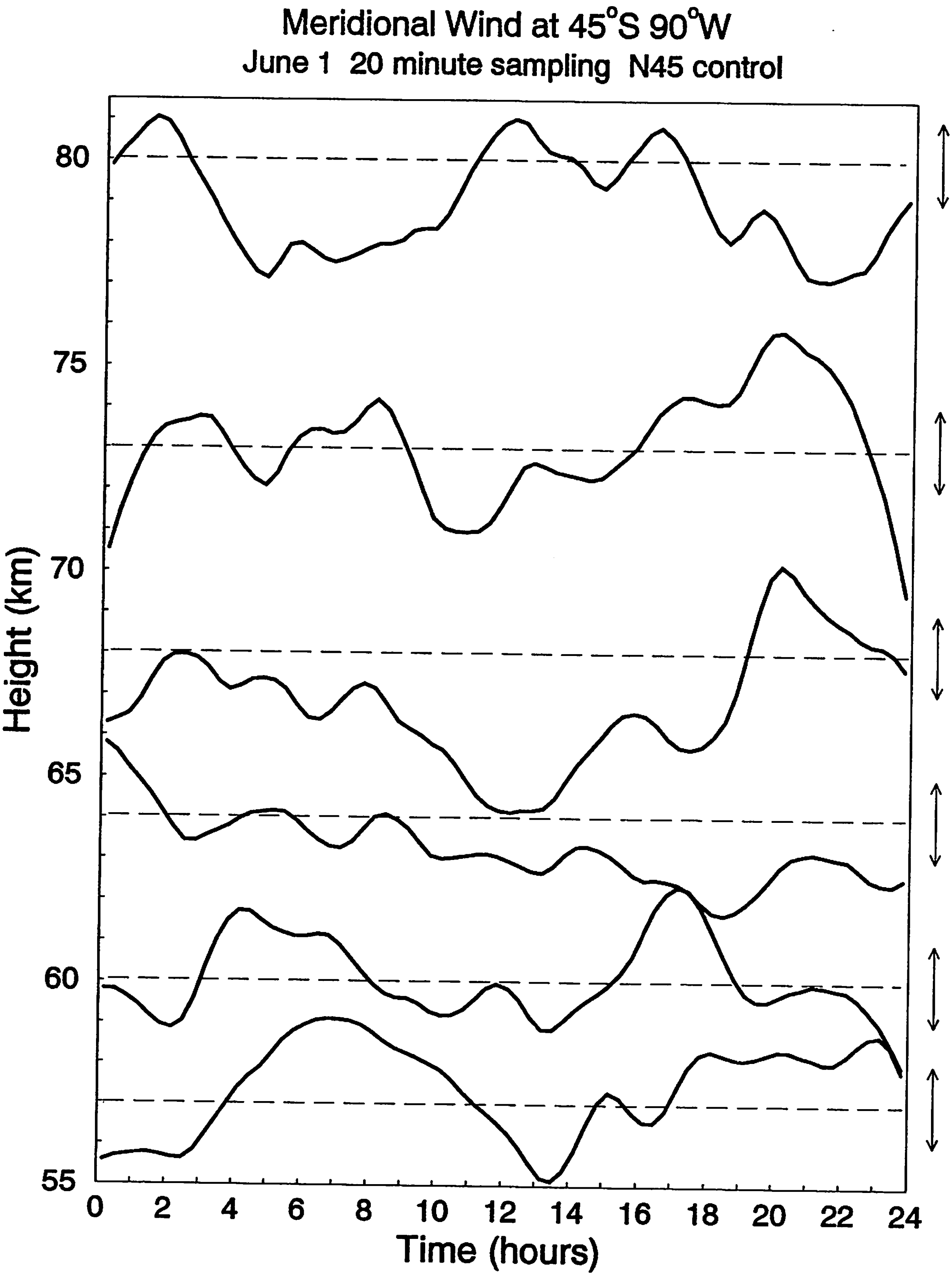

arrow denotes 20 m-s^{-1}

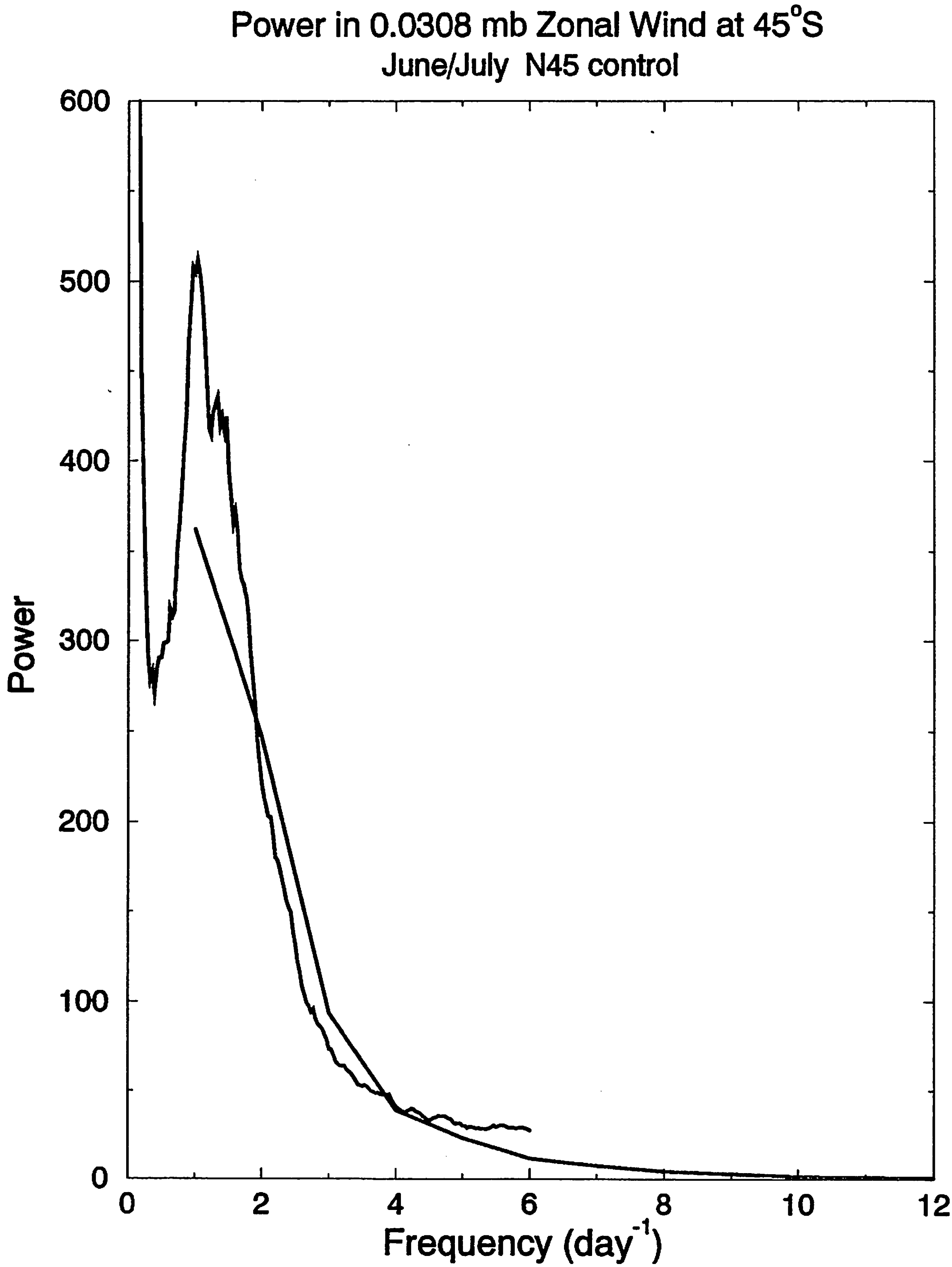
Power in 0.0308 mb Zonal Wind at 45°S
June/July N45 control
600
500
400
300
200
100
0
Power
0
2
4
6
8
10
12
Frequency (day^-1)

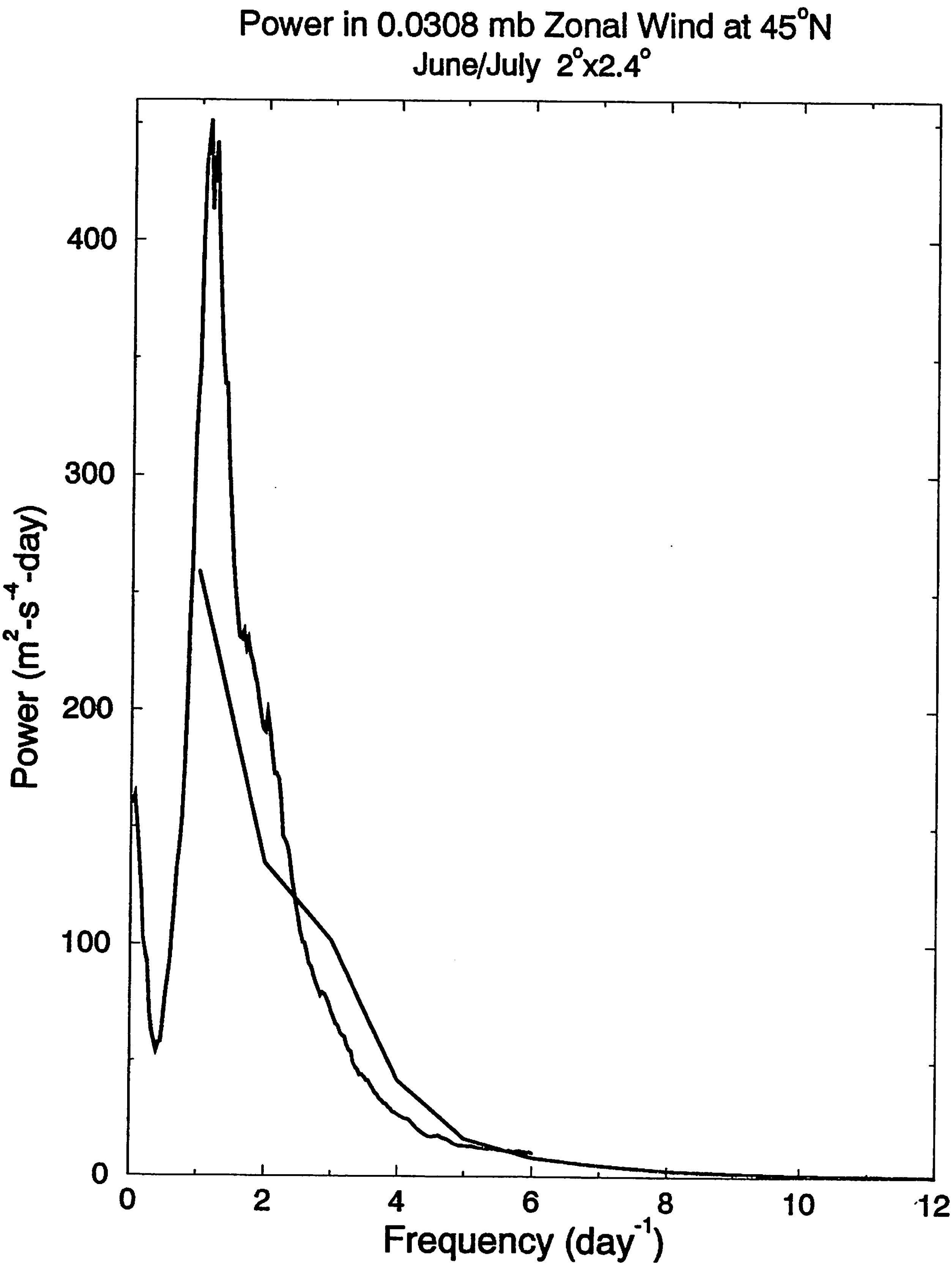
Power in 0.0308 mb Zonal Wind at 45°N
June/July 2°x2.4°
Power (m^2-s^{-4}-day)
400
300
200
100
0
0
2
4
6
8
10
12
Frequency (day^{-1})

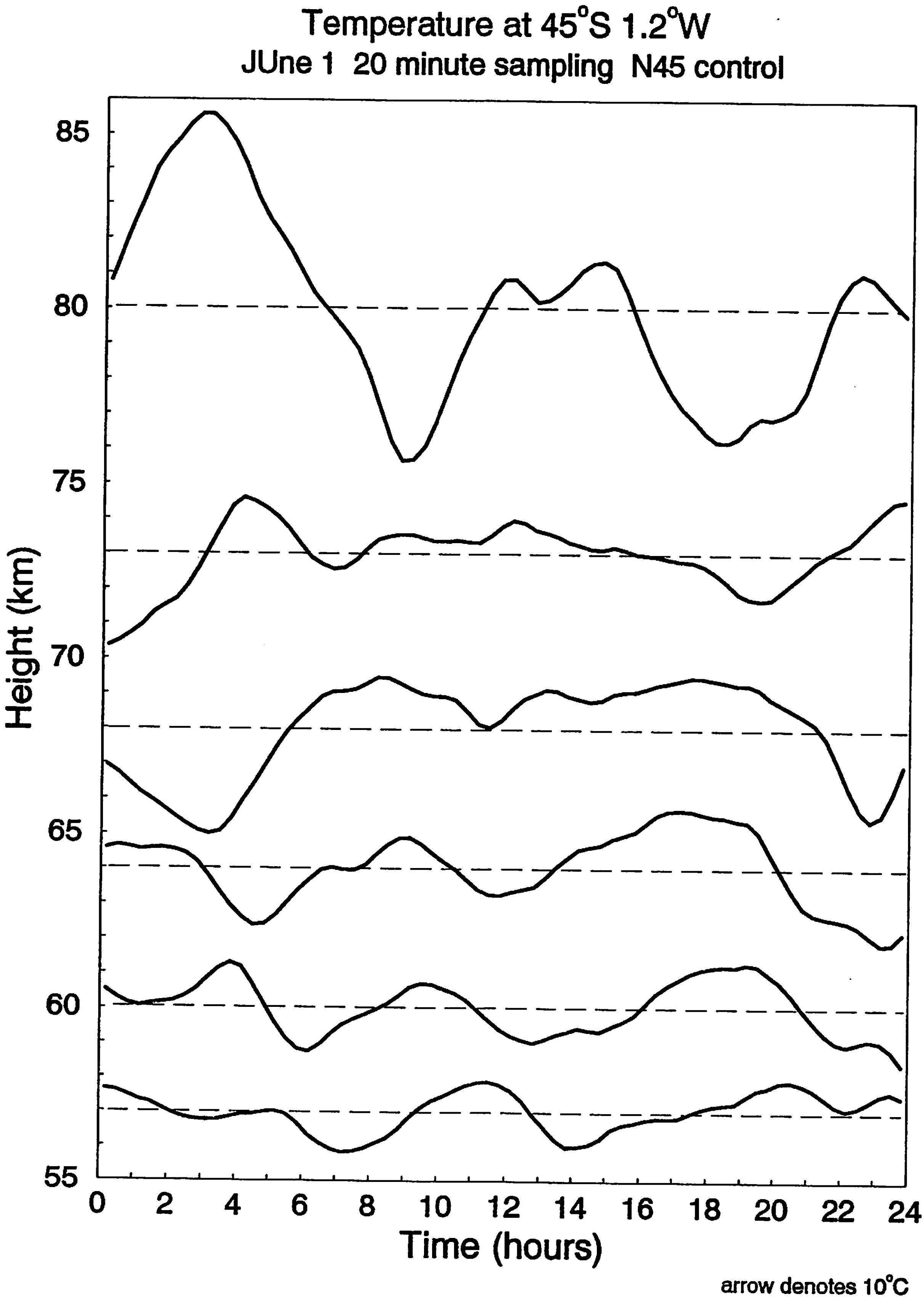
Temperature at 45°S 1.2°W
JUne 1 20 minute sampling N45 control
Height (km)
85
80
75
70
65
60
55
0
2
4
6
8
10
12
14
16
18
20
22
24
Time (hours)
arrow denotes 10°C

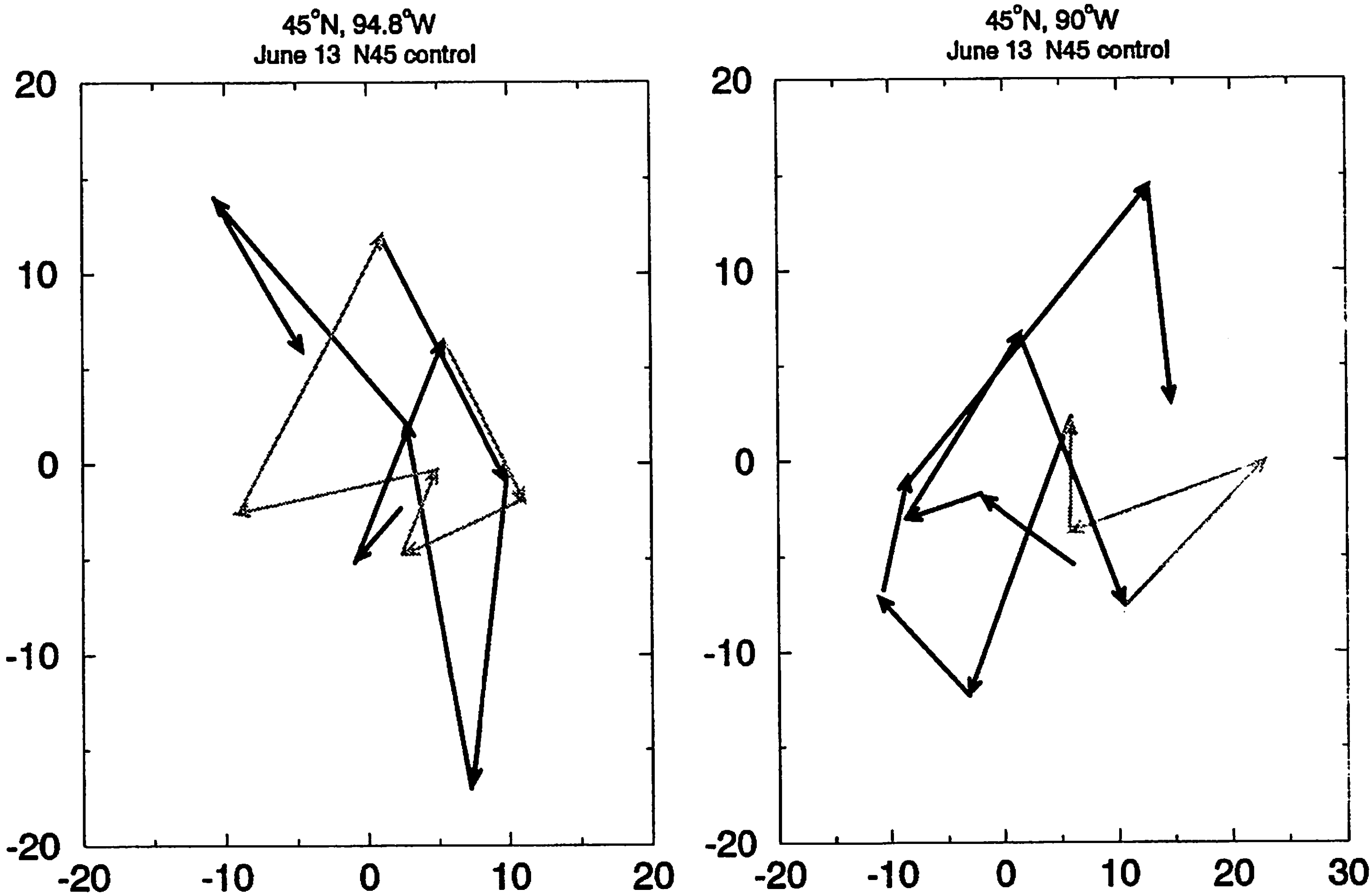
45°N, 94.8°W
June 13 N45 control
45°N, 90°W
June 13 N45 control
20
10
0
-10
-20
-20
-10
0
10
20
30

Hirota and Niki, 1985
Vincent and Fritts, 1987
Eckermann and Vincent, 1989
Eckermann and Hocking, 1989
Hamilton, 1991

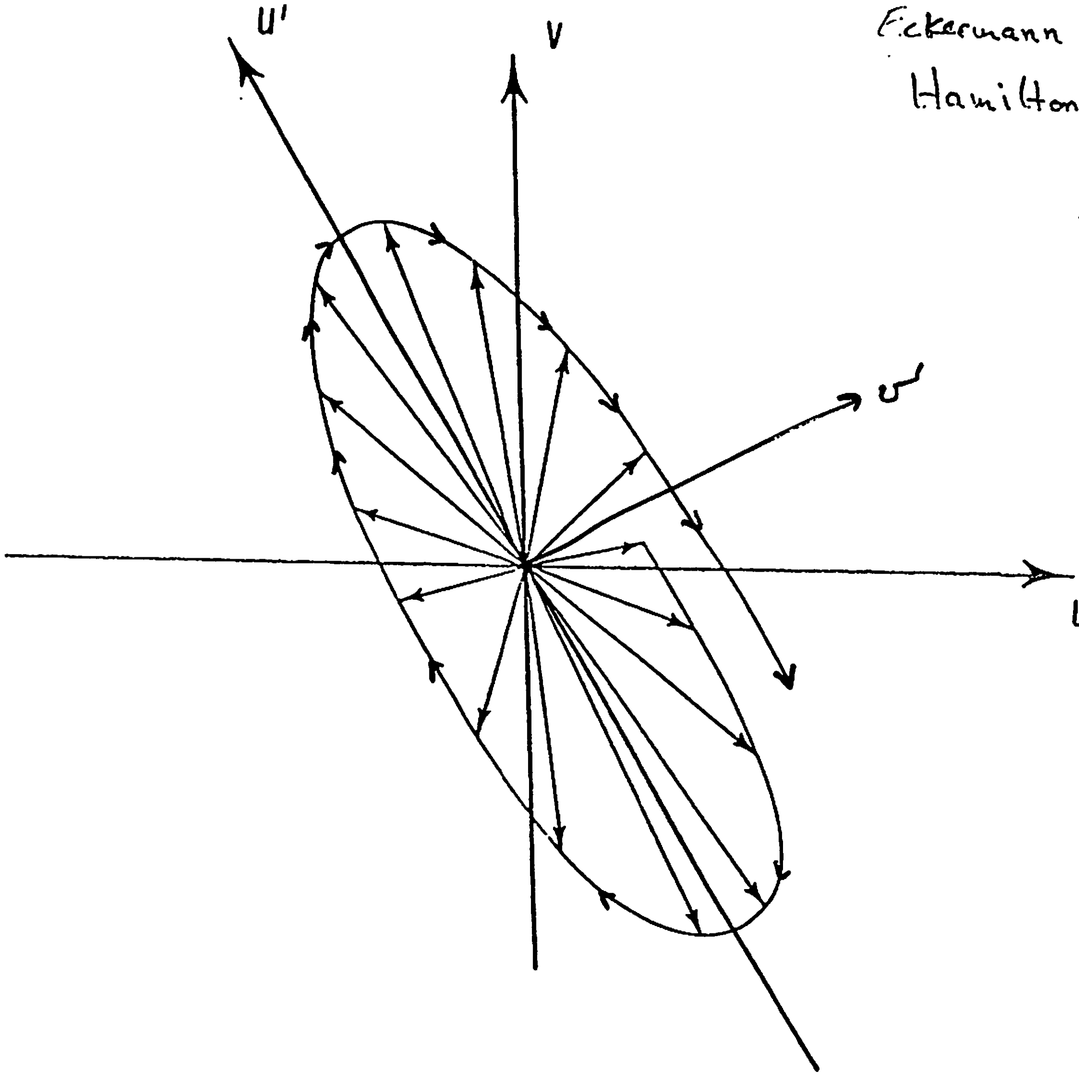

Demand $\overline{u'v'} = 0$ $\overline{u'^2} > \overline{v'^2}$ $\rightarrow$ $\overline{u' \frac{\partial T'}{\partial z}}$ $\rightarrow$ DIR

u Amplitude $\left(\overline{u'^2} + \overline{v'^2}\right)^{1/2}$

T Amplitude $\left(\overline{T'^2}\right)^{1/2}$

Anisotropy $\left(\overline{u'^2}/\overline{v'^2}\right)^{1/2}$

Dominant polarization

u, v, T at 1 km intervals from 28 - 57 km at 12 stations.

	Station	Wind Amplitude (m/s) Observations	Wind Amplitude (m/s) Model	Temperature Amplitude (°C) Observations	Temperature Amplitude (°C) Model
1	Thule 76°N	5.3	2.4	1.8	1.0
3	Churchill 59°N	6.2	3.4	2.1	1.3
5	Wallops. Is. 38°N	5.6	5.7	2.4	1.9
8	Cape Kennedy 28°N	7.8	7.0	2.9	2.2

Station	Average Anisotropy Observations	Average Anisotropy Model	Fraction with Clockwise Polarization Observations	Fraction with Clockwise Polarization Model
Thule 76°N	2.4	5.8	0.98	0.80
Churchill 59°N	2.3	3.7	0.95	0.78
Wallops Is. 38°N	3.0	2.8	0.91	0.96
Cape Kennedy 28°N	2.7	3.8	0.93	0.98

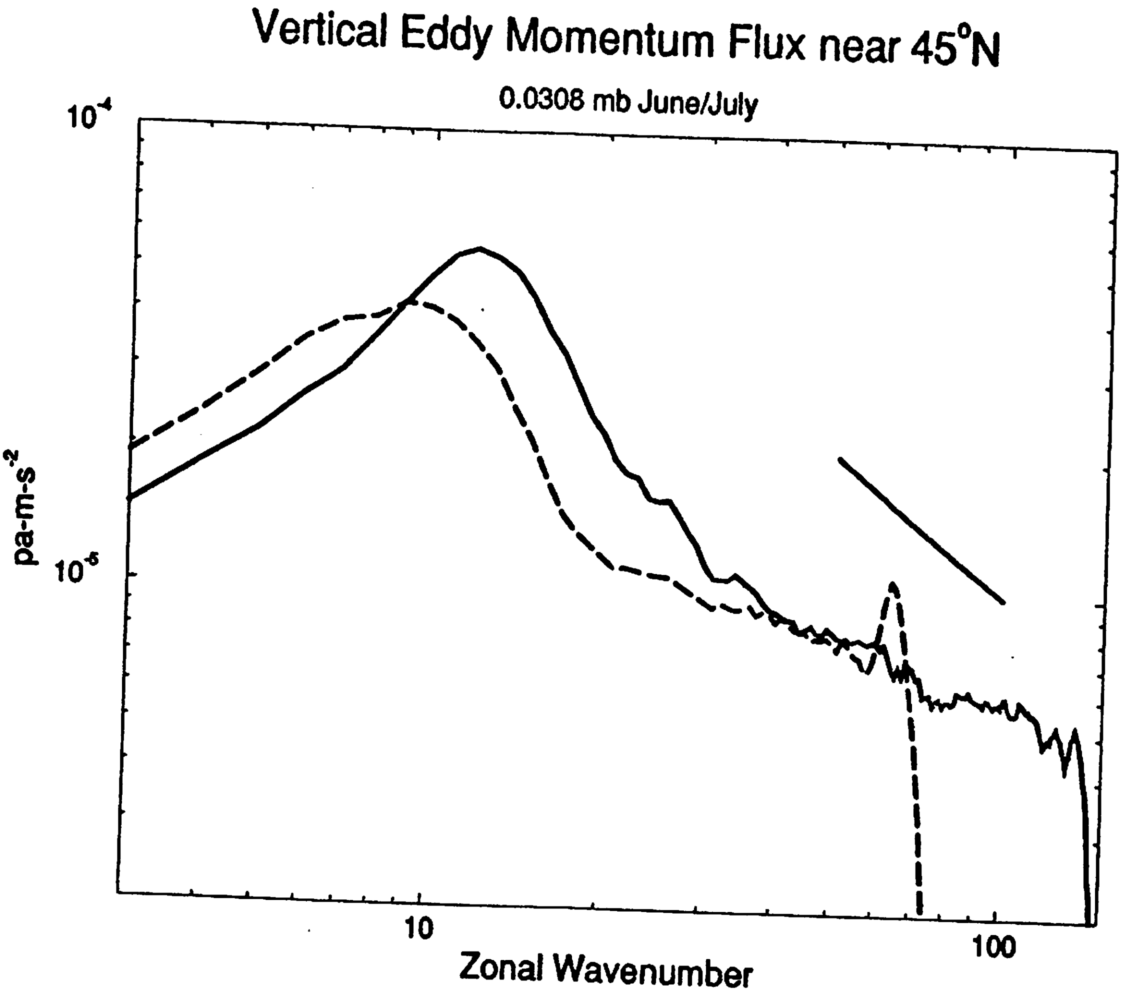

Figure 8. Zonal spectrum of the vertical eddy flux of zonal momentum. Results for the 2^{o}x2.4^{o} model (dashed) and the 1^{o}x1.2^{o} model (solid). In each case the results represent an average over 200 instantaneous values sampled during a ~30 day period near Northern Hemisphere summer solstice. The fluxes plotted are per non-dimensional zonal wavenumber. Note that zonal wavenumber 1 corresponds to a wavelength of 28000 km, while wavenumber 150 corresponds to a wavelength of 188 km. The reference line has a slope of -1.

Mesospheric Gravity Waves

Radar observations indicate lots of activity at timescales of hours to minutes. Typically downward phase propagation and eliptical polarization of the horizontal velocity vector strongly suggestive of inertio-gravity waves.

The frequency spectrum of horizontal wind is typically

$E \sim \omega^{-p}$ where $1<p<2$ (Fritts, 1984)

Suppose c=fixed, $E \sim k^{-p}$, so $\rho_0 u'w' \sim k^{-(p-1)}$

----> "ultraviolet catastrophe"

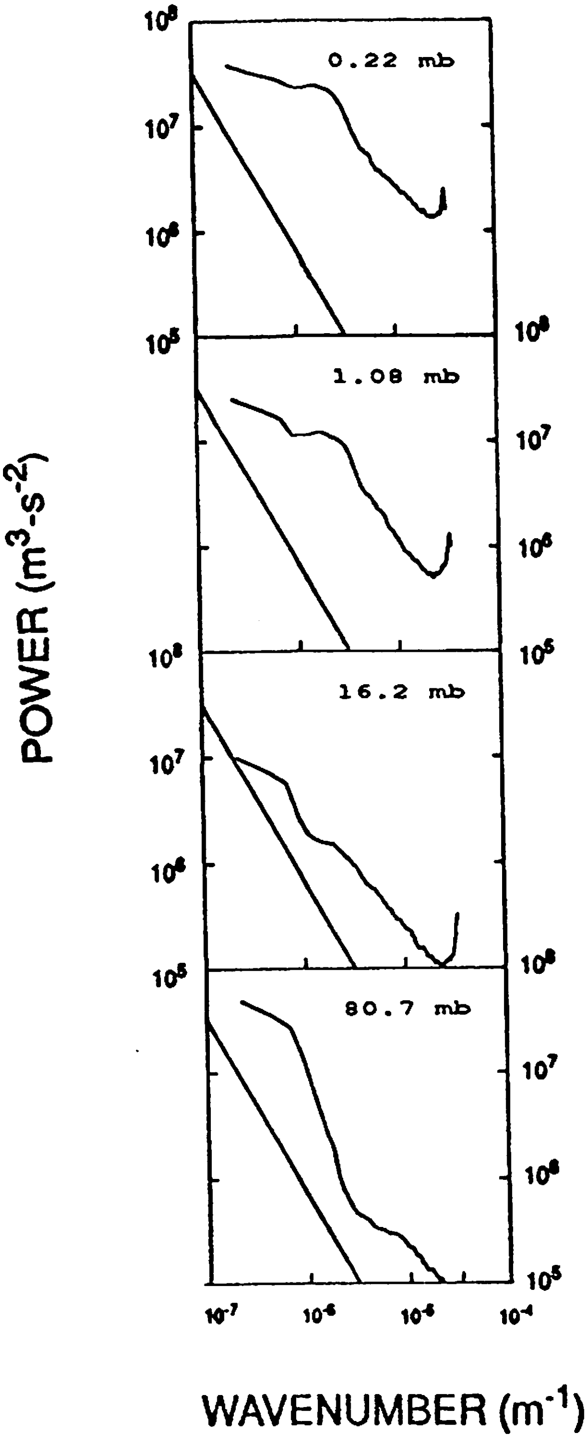

Fig. 5. Power spectral density of the zonal wind along the 44.5°N latitude circle in the N90 SKYHI simulation. Results are presented for four individual isobaric levels and each represents an average of 232 spectra. The straight line has slope -5/3.

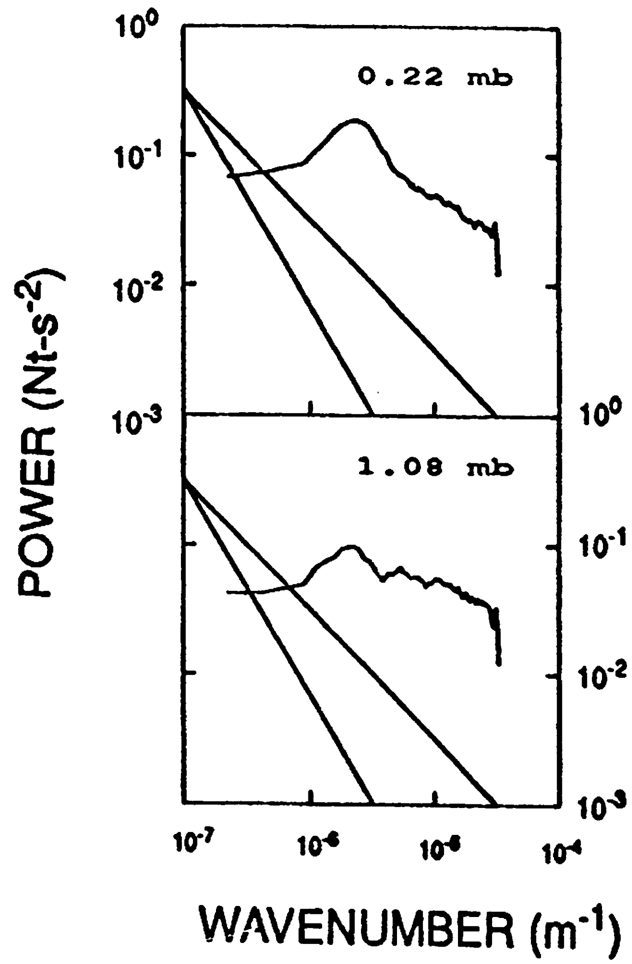

Fig. 6. As in Fig. 5, but for the vertical eddy momentum flux (i.e. minus the cospectrum of zonal wind with the total derivative of pressure). Results only only 0.22 and 1.08 mb. The straight lines have slopes of -1 and -5/3.

POWER SPECTRUM OF EQUATORIAL ZONAL WIND AT 1 mb

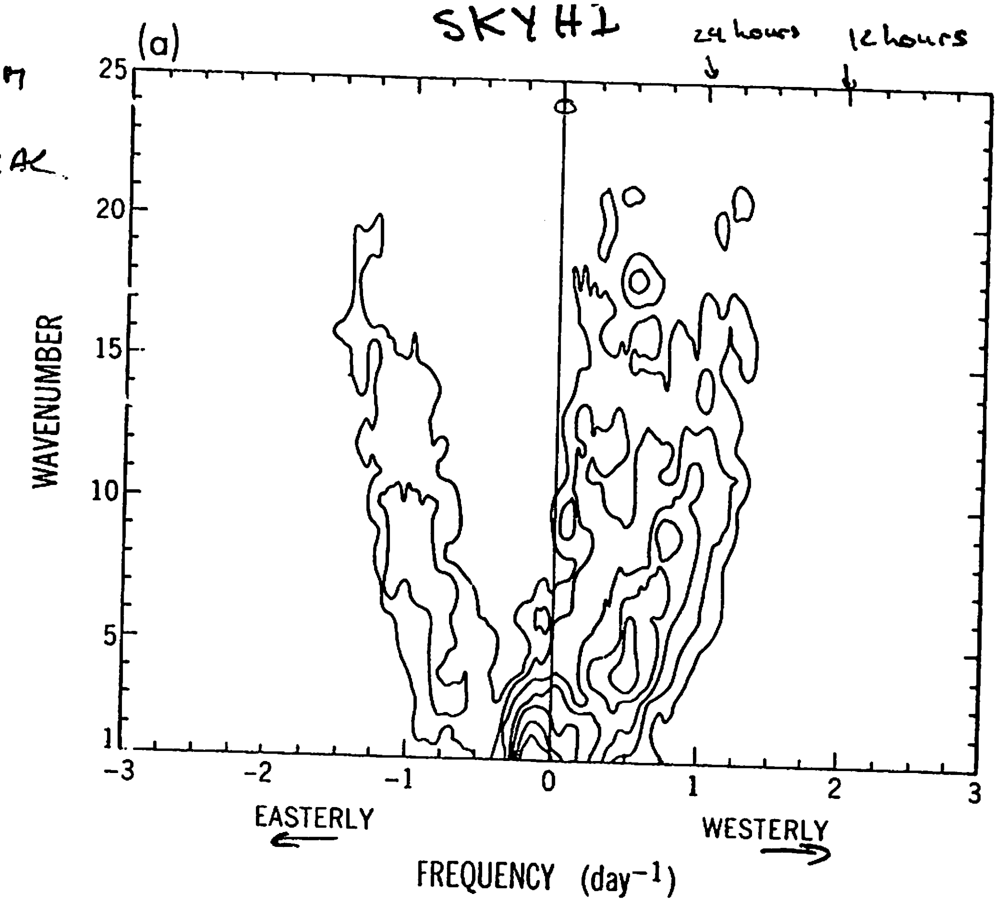

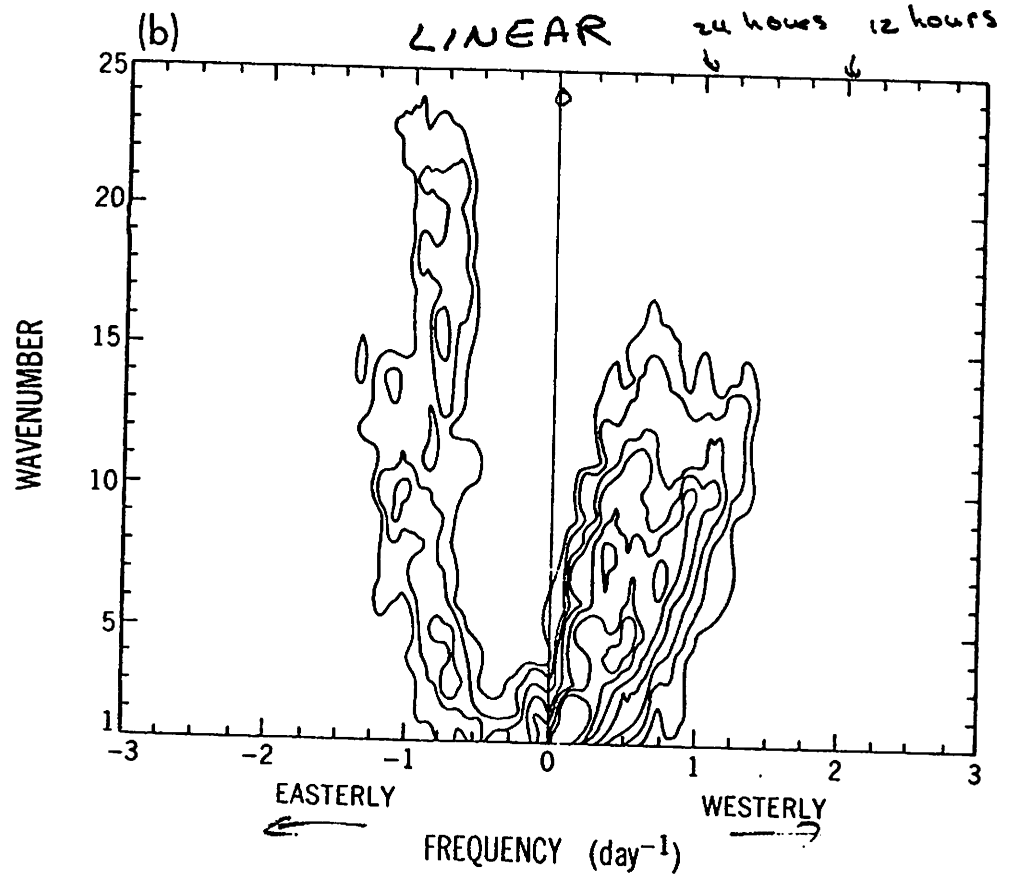

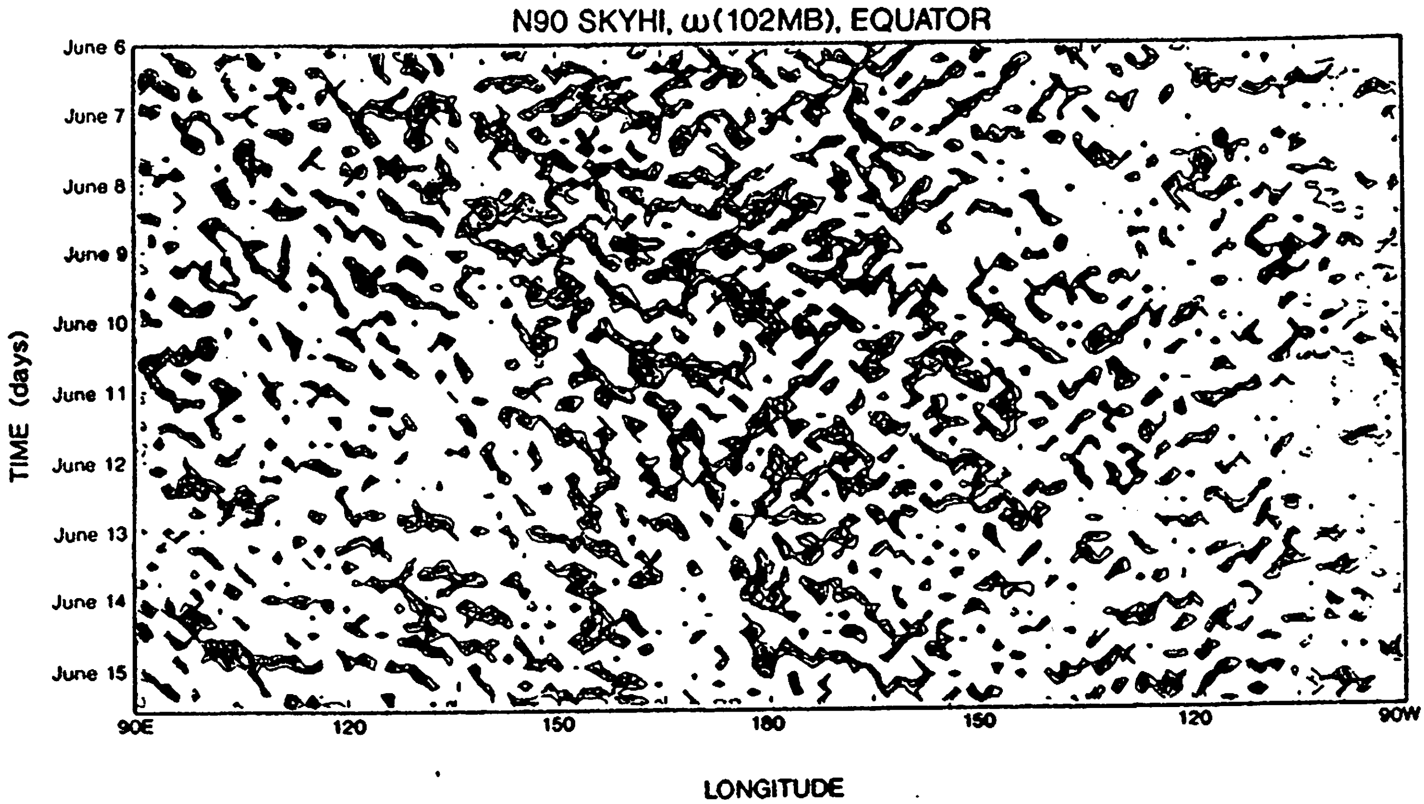
N90 SKYHI, ω(102MB), EQUATOR
June 6
June 7
June 8
June 9
June 10
June 11
June 12
June 13
June 14
June 15
TIME (days)
90E
120
150
180
150
120
90W
LONGITUDE

Time-height Section of Equatorial Zonal Wind at 0° longitude For Easterly Propagating Disturbances with s>4.

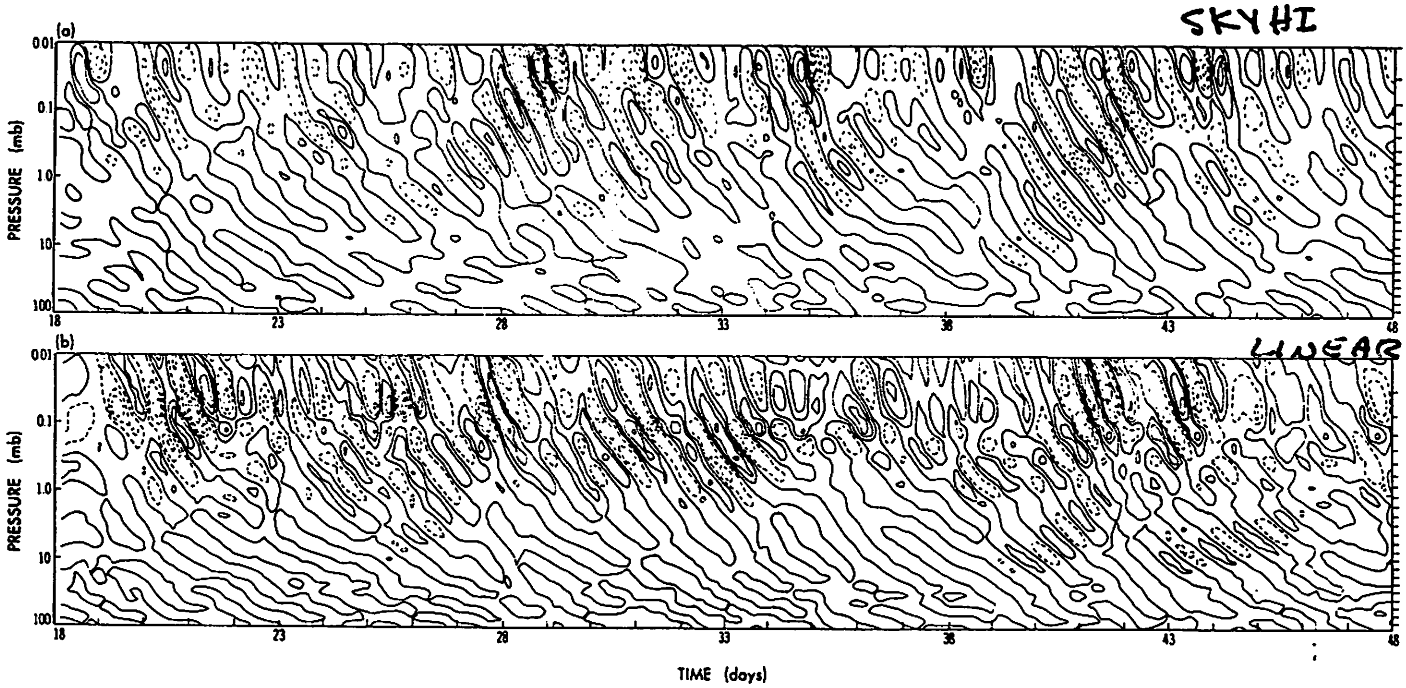

Time-height section of the zonal wind at 30°S and 0° longitude for easterly propagating waves with s>4.

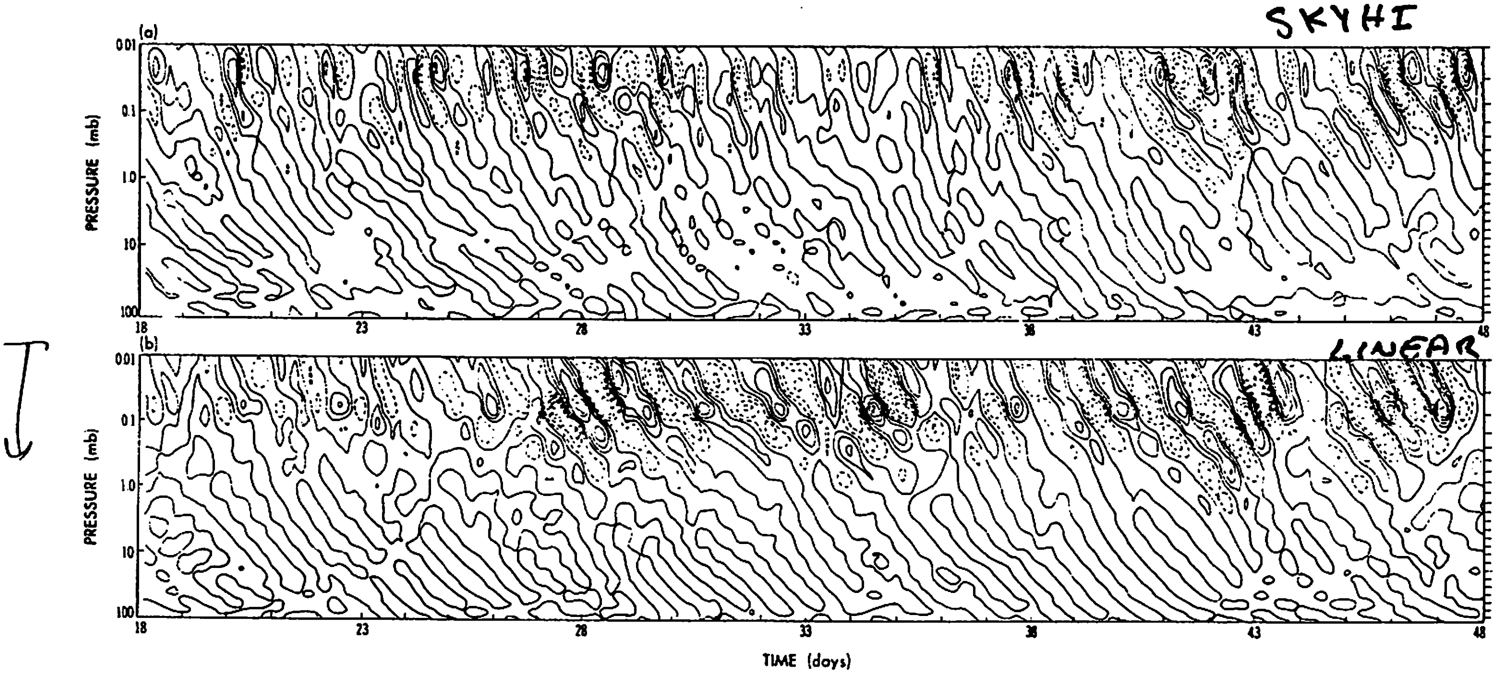

(a)

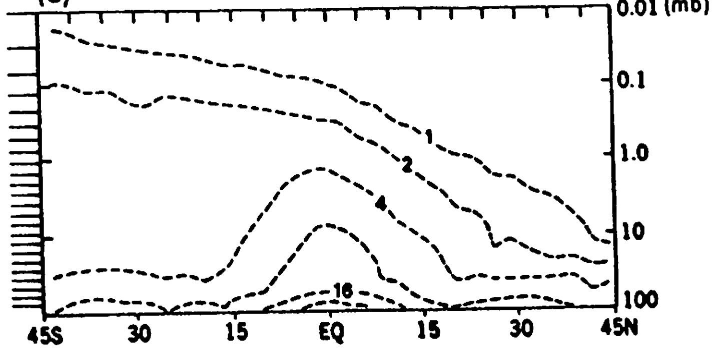
0.01 (mb)
0.1
1.0
10
100
1
2
4
16
45S
30
15
EQ
15
30
45N

(b)

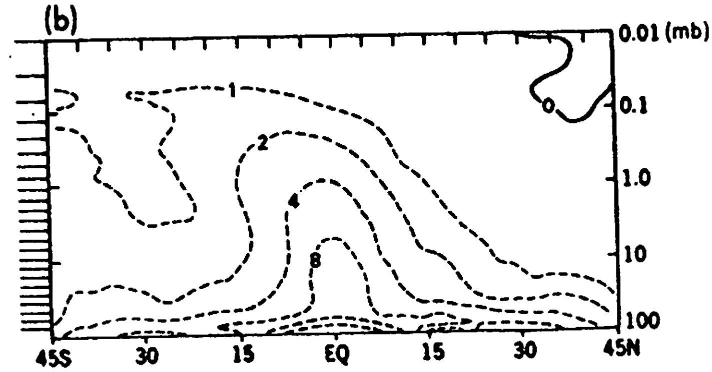
0.01 (mb)
0.1
1.0
10
100
0
1
2
4
8
45S
30
15
EQ
15
30
45N

(b)

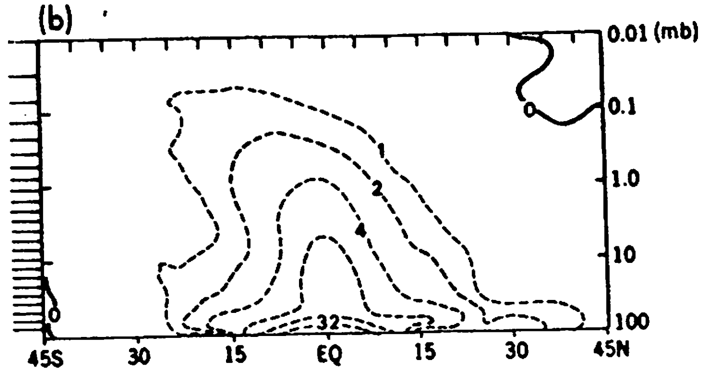
0.01 (mb)
0.1
1.0
10
100
0
1
2
4
32
0
45S
30
15
EQ
15
30
45N

(a)

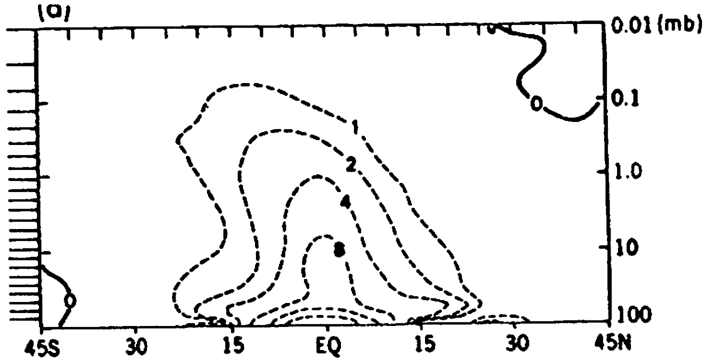
0.01 (mb)
0.1
1.0
10
100
0
1
2
4
8
0
45S
30
15
EQ
15
30
45N

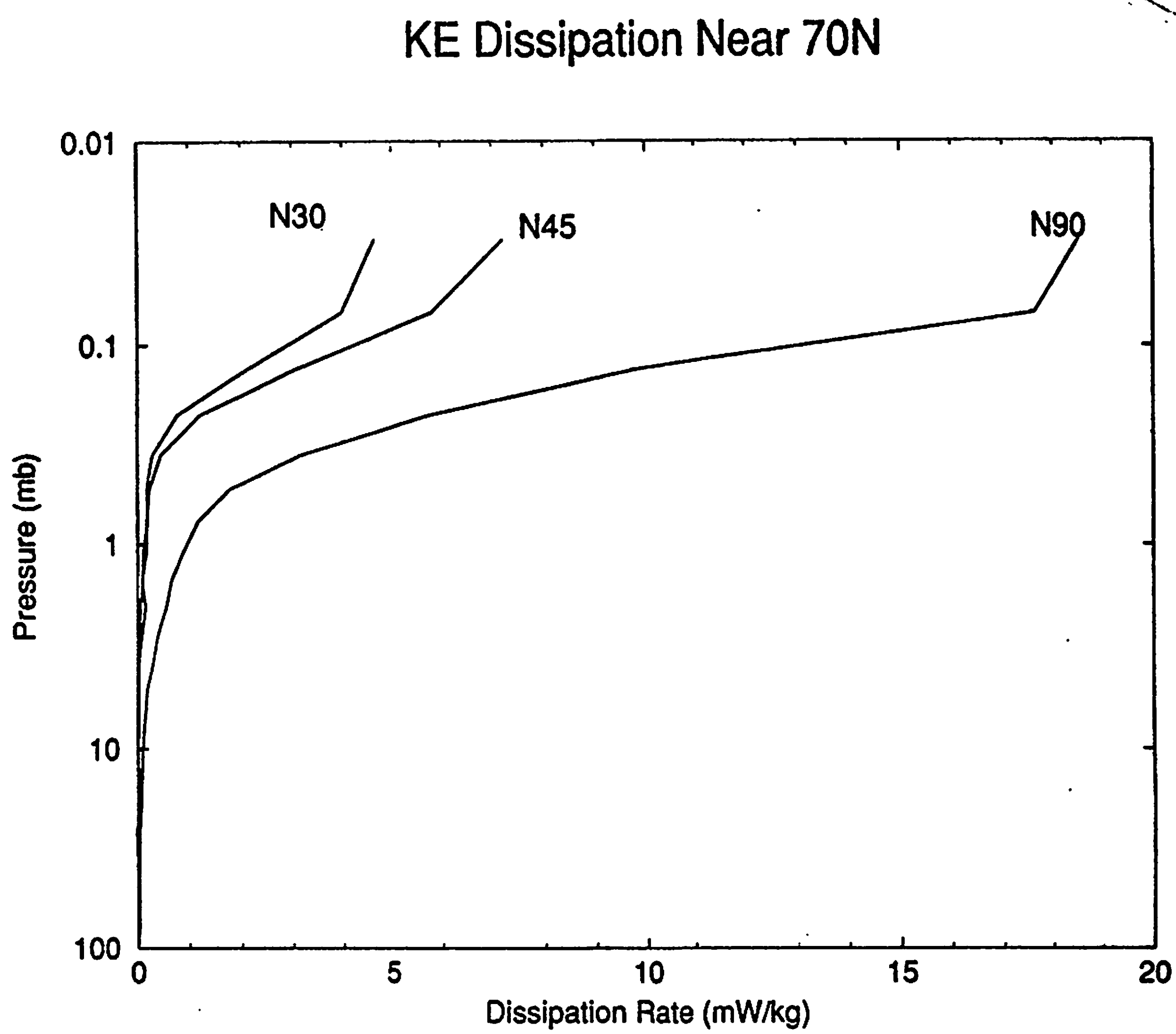

KE Dissipation Near 70N
N30
N45
N90
0.01
0.1
1
10
100
Pressure (mb)
0
5
10
15
20
Dissipation Rate (mW/kg)

Fig. 4

Conclusions

One can construct a comprehensive model with “reasonable” subgrid-scale parameterizations that will produce a good simulation of the time-mean tropospheric circulation

Such a model will produce a middle atmospheric simulation that is driven quite far from radiative equilibrium by both resolved gravity waves and by breaking planetary waves in a midlatitude “surf zone”.

However, typically the result is still unrealistically close to radiative equilibrium, with the winter polar regions being unrealistically cold and the summer mesopause unrealistically warm. These problems are plausibly attributed to the neglect of subgrid-scale gravity waves.

The GFDL SKYHI model produces a middle atmosphere with a great deal of variability over a large range of space and time scales. The higher-frequency part of this variability reflects the presence of a broad spectrum of vertically-propagating gravity waves. By mesospheric levels the global-scale random gravity waves dominate the tide in an instantaneous map of the horizontal winds.

The resolved gravity wave field in SKYHI has some general features that seem to be in accord with observations (e.g. compare with radar obs or UARS Doppler winds). The statistics of the waves in the model have been shown to compare quite well with historical rocket soundings.

The resolved gravity waves have a very shallow spectrum of vertical eddy momentum flux.

The resolved tropospheric latent heating plays a very significant role in the excitation of the resolved waves in the SKYHI middle atmosphere.

The dissipation of kinetic energy in the upper mesosphere in the model is large & may be comparable to observations of the turbulent kinetic energy dissipation in this region.